Journal of Rock Mechanics and Geotechnical Engineering xxx (xxxx) 1–22

Contents lists available at ScienceDirect

Journal of Rock Mechanics and Geotechnical Engineering

journal homepage: www.elsevier.com/locate/JRMGE

Journal Cover Image

Review

Geo-interface modeling with material point method: A review

Tiancheng Xie [a], Honghu Zhu [a,*], Youkou Dong [b], Mingliang Zhou [c], Bin Wang [d], Wei Zhang [a], Jidong Zhao [e]

[a] School of Earth Sciences and Engineering, Nanjing University, Nanjing, 210023, China
[b] College of Marine Science and Technology, China University of Geosciences, Wuhan, 430074, China
[c] Department of Geotechnical Engineering, Tongji University, Shanghai, 200092, China
[d] State Key Laboratory of Geomechanics and Geotechnical Engineering Safety, Institute of Rock and Soil Mechanics, Chinese Academy of Sciences, Wuhan, 430071, China
[e] Department of Civil and Environmental Engineering, The Hong Kong University of Science and Technology, Clear Water Bay, Hong Kong, China

ARTICLE INFO

Article history:
Received 21 February 2024
Received in revised form 30 March 2025
Accepted 1 April 2025

Keywords:
Geo-interface
Material point method (MPM)
Interaction mechanism
Large deformation
Numerical simulation

ABSTRACT

Geo-interfaces refer to the contact surfaces between multiple media within geological strata, as well as the transition zones that regulate the migration of three-phase matter, changes in physical states, and the deformation and stability of rock and soil masses. Owing to the combined effects of natural factors and human activities, geo-interfaces play crucial roles in the emergence, propagation, and triggering of geological disasters. Over the past three decades, the material point method (MPM) has emerged as a preferred approach for addressing large deformation problems and simulating soil-water-structure interactions, making it an ideal tool for analyzing geo-interface behaviors. In this review, we offer a systematic summary of the basic concepts, classifications, and main characteristics of the geo-interface, and provide a comprehensive overview of recent advances and developments in simulating geo-interface using the MPM. We further present a brief description of various MPMs for modeling different types of geo-interfaces in geotechnical engineering applications and highlight the existing limitations and future research directions. This study aims to facilitate innovative applications of the MPM in modeling complex geo-interface problems, providing a reference for geotechnical practitioners and researchers.

1. Introduction

Geo-interfaces are prevalent in both natural and engineered geotechnical environments and serve as critical zones of interaction between different geological strata and/or man-made materials. As illustrated in Fig. 1, geo-interfaces are closely associated with geological hazards and geotechnical failures. Examples include landslides (Alvarado et al., 2019; Hu et al., 2019, 2020; Scaringi and Loche, 2022; Ye et al., 2024; Fang et al., 2024), debris flows (Abe and Konagai, 2016; Tan et al., 2019), levee and dam failures (Zabala and Alonso, 2011; Liang et al., 2020; Girardi et al., 2021, 2023), and tunnel collapse (Deng et al., 2024). They not only act as contact surfaces but also regulate essential geotechnical parameters, such as water content, stress distribution, and overall stability (Zhu, 2023). For instance, the soil cracking interface can facilitate water infiltration, thereby reducing the soil shear strength and potentially triggering shallow landslides (Tang et al., 2021; Zhang et al., 2023b). The catastrophic Xinmo landslide on June 24, 2017 in Diexi town, Mao County, Sichuan Province, China, highlighted the risks associated with neglecting geo-interface monitoring and prediction. Significant deformation in densely vegetated, high-altitude landslide areas went unrecognized, resulting in tragic loss of life and extensive property damage (Scaringi et al., 2018a; Zhao et al., 2021). Therefore, comprehensive identification and detailed analysis of geo-interfaces are essential for predicting and mitigating geological hazards, designing safe and efficient geotechnical structures, and ensuring the long-term stability of engineering projects.

Over the past few decades, extensive theoretical and experimental studies have been conducted on geo-interface behaviors, particularly in slope stability analysis and underground engineering. Various methodologies have been developed, such as block theory (Goodman and Shi, 1985), preferred plane theory (Luo et al., 2003) for rock engineering, and the method of slices for analyzing soil slope stability (Bishop, 1955; Duncan, 1996). Despite these advancements, a complete theoretical framework that fully elucidates the complexities of geo-interfaces is still lacking. In terms of experimental studies, scholars have conducted numerous investigations on the mechanical and hydraulic properties of various geo-interfaces through pull-out, direct shear, simple shear, and ring shear tests (Frost and Han, 1999; Chu and Yin, 2005; Zhu et al., 2011; Scaringi et al., 2018b). These investigations have systematically examined multiple factors that influence the interface shear strength and deformation patterns. Employing advanced testing and monitoring techniques such as X-rays, computed tomography (CT) scans, scanning electron microscopy (SEM), digital image correlation (DIC), distributed fiber optic sensing (DFOS), and the use of transparent synthetic soil, re-

Peer review under responsibility of Institute of Rock and Soil Mechanics, Chinese Academy of Sciences.

* Corresponding author.
E-mail address: zhh@nju.edu.cn (H. Zhu).

https://doi.org/10.1016/j.jrmge.2025.04.001
1674-7755/© 20XX

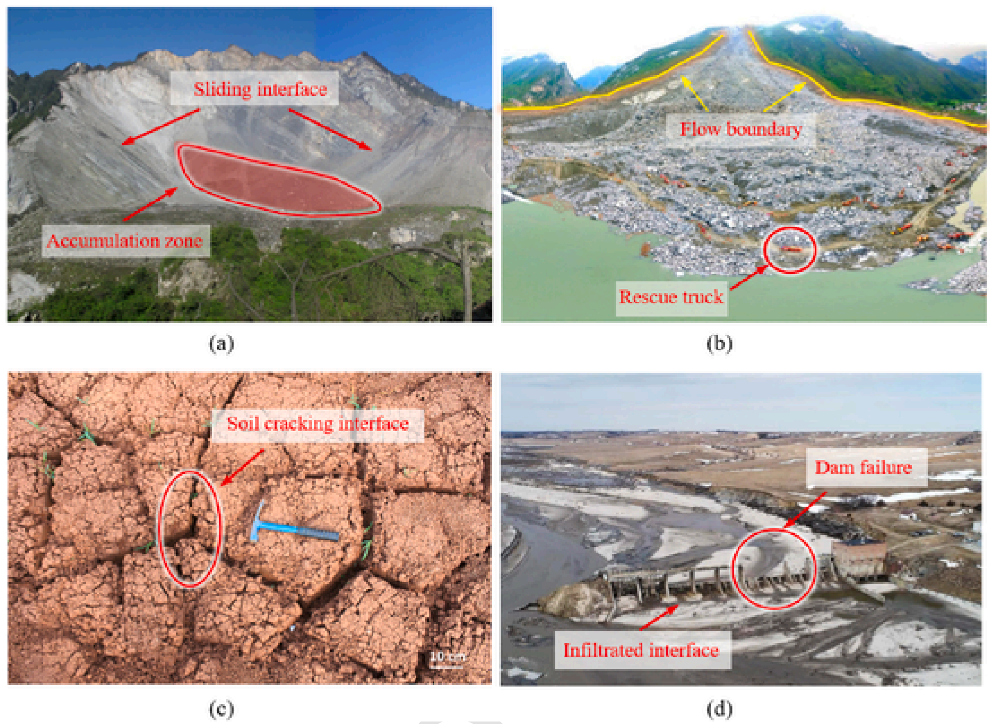

Fig. 1. Photographs of typical geo-interfaces: (a) Exposed sliding surface of the Daguangbao landslide (adapted from Hu et al. (2019) with permission from Elsevier); (b) rescue scene of the Xinmo landslide (adapted from Scaringi et al. (2018a) with permission from Springer); (c) soil cracking interface (adapted from Tang et al. (2021) with permission from Elsevier); and (d) dam failure (adapted from Ettema et al. (2024)).

searchers have achieved detailed visualization and analysis of interface characteristics at micro-to macro-scales (DeJong et al., 2006; Paniagua et al., 2013; Huang et al., 2015, 2021; Hu et al., 2019; King et al., 2019; Wang et al., 2021a, 2024a, 2024b; Ye et al., 2024; Wu et al., 2023). However, a limitation of these studies is that their findings typically apply only to homogeneous or artificially made geo-materials, with failure surfaces often predetermined rather than occurring along the naturally weakest zones. Moreover, discrepancies between laboratory results and field conditions can arise from boundary effects, stress concentrations during loading, and difficulties in controlling drainage conditions, among other factors.

Numerical analysis, validated by experimental and field monitoring data, plays an essential role in deciphering the complexities of geo-interface behaviors. The development of numerical methods such as the finite element method (FEM) and the discrete element method (DEM) has been transformative, offering profound insights into the prediction and comprehension of geo-interface dynamics. Among these advancements, the material point method (MPM) stands out as a powerful hybrid approach (also considered a point-based or meshless approach by many researchers, e.g., Coetzee et al. (2005), Beuth et al. (2011), Ceccato and Simonini (2017), and Liang et al. (2020)). It is specifically designed to address large deformation coupling problems involving soil, rock, water, and structures. The ability of the MPM to accurately model extensive and non-uniform deformations makes it a preferred tool for simulating geo-interface behaviors.

Although the principles and applications of the MPM in geotechnical engineering have been discussed by several researchers (e.g., Soga et al., 2016; Yerro et al., 2022; Ceccato et al., 2024; Zheng et al., 2024), few studies have focused specifically on MPM-based geo-interface modeling. This paper, based on a comprehensive review of the literature, examines recent advances in the MPM for geo-interface simulation. This review provides a detailed classification of geo-interfaces and elucidates the advantages of the MPM in addressing complex geo-interface challenges. The effectiveness of the MPM in simulating large deformations and failures within geo-interfaces is discussed, and some recommendations are provided to improve the modeling performance and accuracy. The relevant research outputs have profound significance for enhancing the effectiveness of geological disaster forecasts and optimizing geotechnical engineering design.

2. Numerical modeling of geo-interfaces

2.1. Classification of geo-interfaces

The geo-interface refers to the contact surfaces between multiple media within geological strata, as well as the transition zones that regulate the migration of three-phase matter, changes in physical states, and the deformation and stability of rock and soil masses (Zhu, 2023). They are categorized into three types: the material interface, the state interface, and the motion interface, as illustrated in Fig. 2. Material interfaces include contact surfaces between geo-materials and man-made continua (e.g., anchors, piles, tunnels, pipelines, retaining walls) and boundaries between adjacent soil and rock layers. State interfaces are characterized by abrupt changes in phase or state parameters (stress, moisture, temperature, etc.), such as wetting fronts generated during rainfall infiltration. Motion interfaces refer to the development of visible failure surfaces or cracks within geo-materials, such as multiple sliding surfaces in a landslide. These geo-interfaces are inherent to geotechnical systems and crucial for engineering safety and stability. They transition from small to large deformations, involve multiple thermal-hydrologic-mechanical factors, and exhibit complex failure modes. Accurately modeling these interfaces poses significant scientific challenges because of their dynamic characteristics and the complexity of their environmental impacts. To mitigate and prevent geological disasters, properly understanding the physical and mechanical properties of

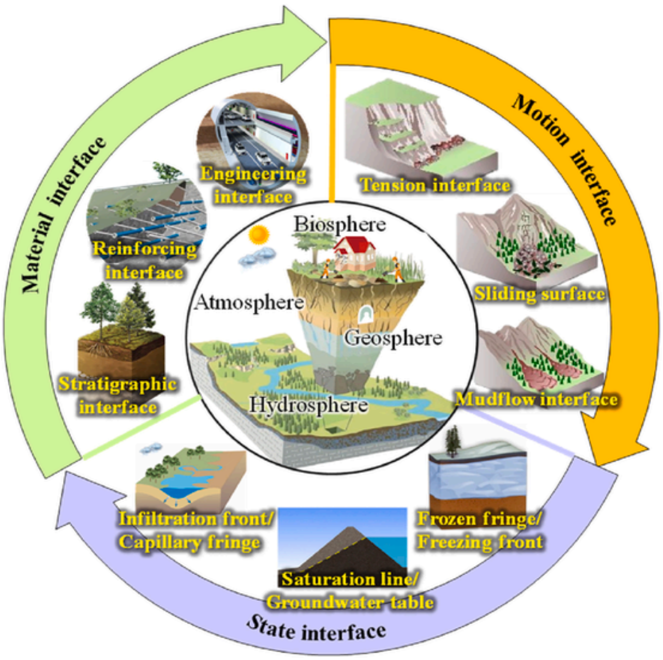

Fig. 2. Schematic diagram of three types of geo-interfaces.

geo-interfaces, along with their catastrophic dynamics, is highly important.

2.2. Comparison of geo-interface modeling approaches

Different numerical methods adopt distinct modeling approaches to analyze geo-interfaces. The FEM and finite difference method (FDM) have been utilized to examine the failure mechanisms of geo-interfaces under various conditions (Chaloulos et al., 2015, 2017; Roy et al., 2018). However, simulating problems involving large deformations poses significant challenges when conventional mesh-based Lagrangian methods are used. Under large deformations, these methods often result in terminated numerical simulations or inaccurate outcomes due to excessive mesh distortion (Wang et al., 2016c; Bisht et al., 2021; Zhao et al., 2022b, 2023a). To address the challenges posed by mesh distortion, various approaches have been employed, such as the coupled Eulerian-Lagrangian (CEL) method, the smoothed particle hydrodynamics (SPH) method, the particle finite element method (PFEM), the DEM, and the MPM. Each of these advanced approaches offers unique benefits and limitations (Chen et al., 2017; Ceccato et al., 2018b; Yuan et al., 2019a; Onyelowe et al., 2023), as summarized in Table 1. Since the MPM is capable of simulating both quasi-static problems and large deformation failures and provides multi-field data, including displacement, velocity, and stress information, this approach has garnered significant attention in the field of geotechnical engineering. Moreover, the MPM can simulate geological disaster chains induced by rainfall, earthquakes, and other factors, effectively capturing failure mechanisms and post-failure behaviors. Consequently, the MPM is recognized as one of the most effective approaches for simulating the evolution of geo-interfaces.

Table 1
Summary of the numerical methods used to model geo-interfaces.

Method	Advantage	Limitation	Example of application
FEM	Capable of incorporating soil constitutive models to simulate changes in stress and deformation at geo-interfaces	Hard to simulate large deformations and post-failure behaviors of geo-interfaces due to mesh distortion	Pipe-soil interaction (Yimsiri et al., 2004); Sliding surfaces in slopes (Kalantari et al., 2023)
CEL	Suitable for handling large deformations at soil-structure interfaces and fluid-solid interactions (Qiu et al., 2011)	Numerical accuracy at geo-interfaces is affected by Eulerian mesh coarseness (Soga et al., 2016)	Soil-structure interaction (Chen et al., 2019); Sliding surfaces in slopes (Chen et al., 2021)
SPH	Capable of simulating fluid-solid interactions and analyzing complex catastrophic behaviors at geo-interfaces (Pastor et al., 2018)	Requires special boundary approaches at geo-interfaces and low computational efficiency due to searching particles (Qin et al., 2022)	Infiltration front (Zhang et al., 2016a); Mudflow interface (Pastor et al., 2021)
PFEM	Suitable for handling large deformation problems and fluid-solid coupling at geo-interfaces (Chen et al., 2017)	Requires special contact approaches at geo-interfaces (Soga et al., 2016)	Fluid-structure interaction (Yuan et al., 2019b); Pipe-soil interaction (Yuan et al., 2021)
DEM	Useful for simulating the microstructure and dynamics of geo-interfaces	Requires many assumptions and is computationally expensive when simulating complex geo-interfaces (Zhao et al., 2021; Qin et al., 2022)	Sliding surfaces in slopes (Xia et al., 2021); Soil cracking interface (Le et al., 2022)
MPM	Suitable for simulating large deformation problems with complex geo-interfaces (Soga et al., 2016)	Numerical errors may occur at geo-interfaces due to the cell-crossing noise (Soga et al., 2016; Qin et al., 2022)	Sliding surface in slopes (Ceccato et al., 2024); Soil-water interaction (Martinelli et al., 2020); Pipe-soil interaction (Zhang et al., 2022a, 2023a)

3. Material point method

3.1. Historical development and scientometric analysis

The history of the MPM is shown in Fig. 3. Over the past three decades, the utilization of MPM has increased significantly in the fields of geotechnical and geological engineering for studying soil-water-structure problems (Coetzee et al., 2005; Phuong et al., 2016; Kiriyama and Higo, 2020; Acosta et al., 2021a; Li et al., 2021b; Zhang et al., 2022b; Chen et al., 2023; Tu et al., 2023). By combining the benefits of the Eulerian and Lagrangian methods, the MPM can achieve accurate numerical solutions for various geotechnical issues without mesh distortions. An increasing number of boundary conditions and coupling algorithms have been developed to increase the accuracy of geo-interface MPM modeling (Shen and Chen, 2005; Beuth, 2012; Al-Kafaji, 2013; Liang and Zhao, 2019; Chen et al., 2023; Yu et al., 2024). To better demonstrate the development of MPM, a scientometric analysis was conducted using specific keywords in the Web of Science database. The procedures for conducting scientometric analysis generally follow those elucidated in Hosseini et al. (2018), Tariq et al. (2021), and Huo et al. (2023). Following the completion of the bibliometric search and scientometric analyses, there were 680 publications in the field of engineering in total, of which 312 were related to geo-interfaces (Fig. 4). While constraints such as search methods, keywords, and database limitations might have excluded some related publications (Zhang et al., 2023c), this statistic provides useful insights into the development trend of MPM within the geo-engineering field, particularly highlighting the rapid advancement in geo-interface modeling.

3.2. Computational principles and applications

In the MPM calculation process, the continuum is discretized into a series of material points (MPs). Each MP represents a material subdomain and contains all pertinent physical information, such as density, velocity, stress, and material parameters (Zhang et al., 2016b; Fern et

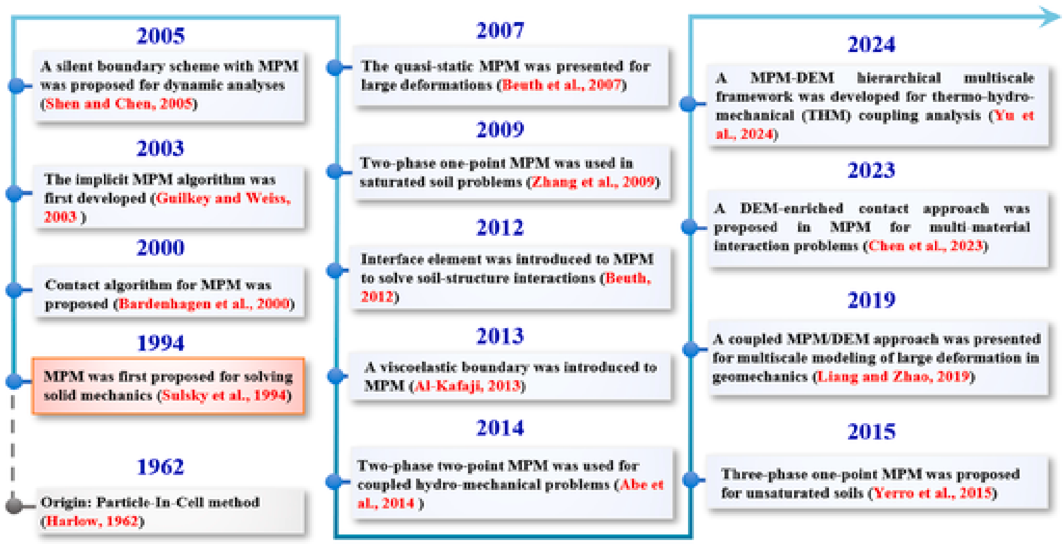

Fig. 3. Brief history of the MPM.

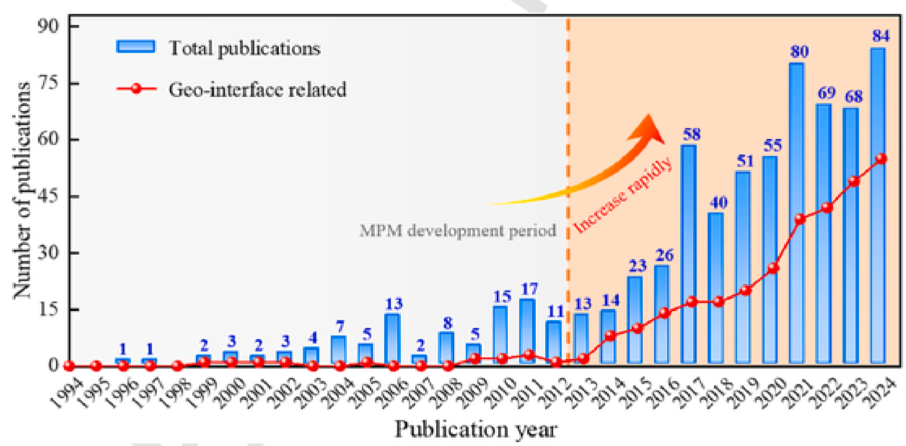

Fig. 4. Annual distribution of research publications related to the MPM (Database: Web of Science Core Collection; Keywords: Material Point Method or MPM in the title of publications; Research Area: Engineering).

al., 2019; Nguyen et al., 2022; Yildizdag, 2023). The background mesh covers the entire computational domain, not only the shape of the modeling body. The information carried by these MPs is mapped to the Eulerian background grid, which is used to solve the field balance equations (Yang and Qiu, 2020; Ceccato et al., 2024). Fig. 5 shows a schematic diagram of the MPM computational steps. The time increment in the MPM typically involves four calculation steps (Xie et al., 2023, 2024a; Zhu et al., 2023). First, all the material information is mapped to the Eulerian background grid via the shape function. Second, nodal momentum equations are formulated and solved to obtain new physical variables. Third, the state variables are mapped back to the MPs, and the accelerations and velocities of the MPs are updated. Finally, the positions of the MPs are updated, and the mesh is restored to its original configuration. Since the focus of this review is on MPM modeling of geo-interfaces, the governing equations and fundamental principles of the MPM algorithm have been omitted. Detailed information on these topics can be found in the literature (Al-Kafaji, 2013; Zhang et al., 2016b; Fern et al., 2019; de Vaucorbeil et al., 2020).

Fig. 6 depicts the solution of a representative geotechnical issue involving a large deformation slope collapse, as analyzed using both the traditional FEM and the MPM. The comparison suggests that the FEM experiences significant mesh distortions, whereas the MPM allows for a more comprehensive simulation of slope collapse (Llano-Serna et al., 2016; Li et al., 2016; Yerro et al., 2016; Shi et al., 2018, 2019; Conte et al., 2019, 2020; Lee et al., 2019a, 2019b, 2021; Cuomo et al., 2021c, 2023; Ying et al., 2021; Liu et al., 2021, 2022; Ceccato et al., 2024). Furthermore, considering that many geotechnical applications involve multi-phase interactions and geological activities, such as rainfall-induced landslides (Wang et al., 2016a, 2016b, 2018; Liu et al., 2020; Cuomo et al., 2021c; Liu and Wang, 2021; Feng et al., 2021; Zhu et al., 2022; Lu et al., 2023), embankment collapses due to seepage or wetting (Zabala and Alonso, 2011; Fern et al., 2017; Martinelli et al., 2017a), and seismic slope failures (Bhandari et al., 2016; He et al., 2019), the MPM has substantial applications in the analysis of two- or three-phase large deformation simulations, particularly in scenarios involving phase transitions at geo-interfaces (Yerro et al., 2015, 2022; Bandara et al., 2016; Martinelli, 2016; Dong et al., 2017b, 2020a; Martinelli et al., 2017b; Li et al., 2022; Liang et al., 2022, 2023a; Monzer et al., 2023; Zhan et al., 2023). When combined with specific contact algorithms, the MPM can also be extended to address large deformations and dynamic contact behavior at soil-structure interfaces, such as pipe-soil interactions (Zhang et al., 2022a, 2023a; Zhu et al., 2023; Xie et al.,

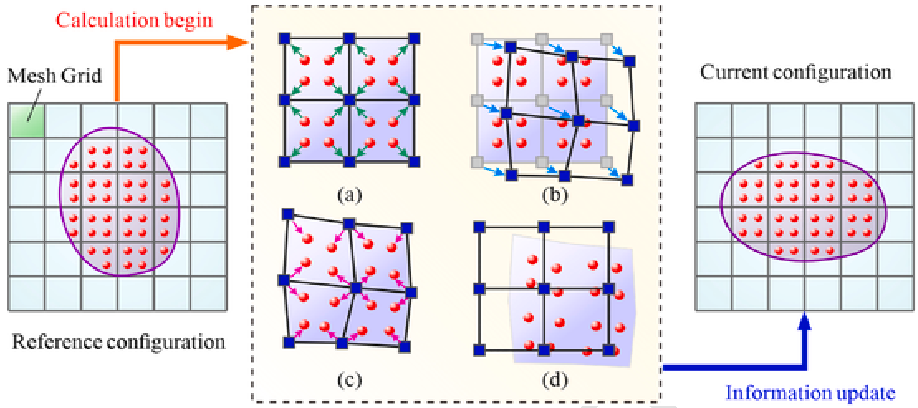

Fig. 5. Schematic illustration of the MPM.

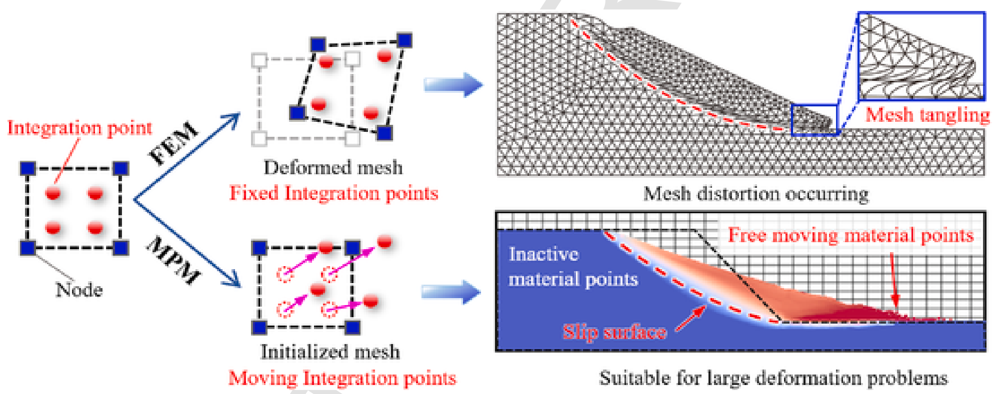

Fig. 6. Comparison of geo-interface simulations between the FEM and MPM.

2024a), landslide-structure interactions (Mast et al., 2014; Dong et al., 2015, 2017a, 2020b; Dong, 2020; Li et al., 2020; Acosta et al., 2021b; Cuomo et al., 2021a, 2021b, 2022; Perna et al., 2022a, 2022b; Vicari et al., 2022), and soil-tunnel interactions (Xie et al., 2022; Li et al., 2023b; Tu et al., 2023).

Table 2 summarizes the common categories and variations of the MPM with respect to basis/shape functions, time integration schemes, and mesh type. When MPs cross grid boundaries, the standard MPM suffers from cell-crossing instability. In an attempt to remedy this issue, researchers introduced several advanced approaches based on different grid basis functions, such as the generalized interpolation material point (GIMP) method (Bardenhagen and Kober, 2004), in which the characteristic function was introduced to construct the particle domain; the B-spline material point method (BSMPM) (Steffen et al., 2008; Zhang et al., 2023a), in which higher-order nodal shape functions were adopted; the convected particle domain interpolation (CPDI) (Sadeghirad et al., 2011, 2013; Kiriyama and Higo, 2020), in which the shear and rotational deformation of the control domains could be considered; and the dual domain material point (DDMP) method (Zhang et al., 2011), in which the gradient of the shape functions was modified and smoothed.

The MPM can be categorized into explicit, implicit, and semi-implicit forms on the basis of different time integration schemes (Fern et al., 2019). The explicit MPM is efficient for dynamic simulations but is limited by stringent time-step requirements (Bandara and Soga, 2015). The implicit MPM allows for larger time steps and enhanced stability but requires solving large systems of equations at each step, increasing computational complexity and cost, which can potentially pose convergence challenges (Guilkey and Weiss, 2003). The semi-implicit MPM combines the advantages of explicit and implicit methods, offering larger time steps and improved computational stability while reducing computational costs, making it increasingly favored by researchers (Liang et al., 2023a). Furthermore, a Cartesian grid (e.g. a regular/structured tetrahedral mesh) is usually used in the MPM to eliminate the need for computationally expensive neighborhood searches during particle-mesh interactions (Zhang et al., 2022a). In contrast to the Cartesian grid, searching for which element contains a given particle in an unstructured grid is very time-consuming. However, the use of an unstructured grid facilitates the enforcement of complex boundary conditions (i.e. boundary conditions on curved surfaces) (de Vaucorbeil et al., 2020).

3.3. *Geo-interface modeling challenges*

In modeling geo-interfaces with the MPM, accurately handling contacts between different bodies and imposing appropriate boundary conditions are key challenges. Compared with the MPM, the mesh structure of the FEM provides a clear representation of boundaries, making the application of boundary conditions more straightforward. However, the treatment of boundary conditions in the MPM often involves mapping between the mesh and MPs, which necessitates the adoption of special strategies to simulate complex boundary conditions. To address these issues, researchers have proposed a variety of approaches. Zhao et al. (2023c) leveraged the level set method to address geo-interface issues with complex shapes and combined it with the barrier method to simulate contact (Zhao et al., 2022c). This ensured that the particles could

Table 2
Overview of several common MPM variants.

Classification	MPM variant	Source	Description
Basis/shape functions	Standard MPM	Sulsky et al. (1994)	Suffers from the cell-crossing instability
	GIMP	Bardenhagen and Kober (2004); Andersen and Andersen (2010)	An effectively remedy for the cell crossing issue; Specific calculation domain may lead to the GIMP suffering from low accuracy
	B-splines MPM	Steffffen et al. (2008); Zhang et al. (2023a)	Another popular approach to reduce the cell-crossing error
	CPDI	Sadeghirad et al. (2011, 2013); Kiriyama and Higo (2020)	Enhances the accuracy of the GIMP under arbitrary deformations
	DDMP	Zhang et al. (2011)	Not necessary to construct a new basic shape function; Not easy to converge when the number of particles is small
Time integration schemes	Explicit MPM	Bandara and Soga (2015); Conte et al. (2020)	The most common scheme of the MPM; Easy to implement, efficient and stable for short duration dynamic problems
	Semi-implicit MPM	Liang et al. (2023a); Yuan et al. (2023)	Allows for larger time steps and more convenient stability properties
	Implicit MPM	Guilkey and Weiss (2003); Acosta et al. (2021a)	Suitable for low strain rate and quasi-static problem; Computationally expensive
Grid types	Cartesian grid	Zhang et al. (2022a); Xie et al. (2024b)	Reduces the computational cost of neighborhood searches during particle-mesh interaction
	Unstructured grid	Więckowski (2004); Zhu et al. (2023)	Time-consuming; Facilitates the enforcement of complex boundary conditions

not penetrate the mesh throughout the simulation process. This approach has been verified and demonstrated to be effective in simulating geo-interface issues, where soils interact with complex rigid bodies. However, when the level set method is used in conjunction with an implicit integration scheme in the MPM, it may increase the complexity and cost of calculations. To address the misalignment between material boundaries and mesh boundaries in the MPM, Liang et al. (2023b) and Given et al. (2024) employed the virtual stress boundary (VSB) method to impose nonconforming Neumann boundary conditions. This approach transforms the original boundary traction problem into an equivalent problem featuring a virtual stress field, thereby eliminating the need for explicit boundary positions. Note that both the level set method (Zhao et al., 2023c) and the VSB method can address nonconforming boundaries under different circumstances. The level set method is suitable for fixed surface boundaries within the mesh domain (i.e., the material domain may not always be in contact with some fixed interface, such as fixed background terrain), whereas the VSB method is designed for adaptive surface boundaries where the virtual stress field is applied to all surface materials within a specified bounding box (i.e., the traction changes with the geometry, such as in hydrostatic pressure scenarios). When the VSB method is employed, the magnitude of stress errors decreases with mesh refinement, but the rate of convergence tends to stagnate (Steffen et al., 2008; Charlton et al., 2017). Future research should prioritize enhancing numerical accuracy and gaining a deeper understanding of the factors contributing to stagnating convergence rates.

Additionally, traction loads can be applied to either the element boundaries or the MPs in the MPM. The first option is applicable when the boundary of the body remains aligned with loaded element boundaries throughout the computation (Yerro et al., 2022). This typically necessitates the use of a moving mesh technique to ensure that the boundary of the physical domain remains aligned with the computational mesh. Note that in the more general case of MPM interfaces, the contact interface can remain constant in terms of the nodal definition within a fixed mesh, without always being in contact with the material domain boundary. The second option involves storing the load on selected MPs that move through the mesh. This load is mapped from boundary MPs to all nodes of the element where they are located using shape functions (Yerro et al., 2022). However, this approach requires mesh refinement; otherwise, it may adversely affect MPs that are not located on the boundary (Fern et al., 2019). Moreover, this approach has a notable drawback: when MPs move a long distance from their original positions, it may become inappropriate for them to have boundary conditions applied (Yerro et al., 2022).

In numerical simulations involving wave propagation problems, the use of finite boundaries leads to wave reflection when the waves reach the boundaries of the mesh. These reflecting waves are numerical artifacts and are not physical. Therefore, attenuating wave reflection is necessary in problems where there are artificial boundaries (Al-Kafaji, 2013). One of the most common approaches to address this issue is the implementation of absorbing boundaries. The absorbing boundary is implemented by applying viscous damping forces (dashpots) along the artificial boundary (Lysmer and Kuhlemeyer, 1969; Fern et al., 2019). Al-Kafaji (2013) improved this method in MPM by replacing dashpots with Kelvin-Voigt elements to control creep at the boundaries. Additionally, periodic boundary conditions help reduce artificial wave reflection in numerical simulations and can be used to simulate the coseismic site response and slope instability (Alsardi and Yerro, 2023). However, owing to the requirement for a smaller element size, the use of periodic boundaries may require a trade-off between computational accuracy and computational cost.

Notably, the MPM also encounters numerical challenges such as volumetric locking and the implications of various smoothing methods. However, a detailed discussion of these issues is beyond the scope of this work, which focuses on illustrating the applicability of the MPM in geo-interface simulations.

3.4. Geo-interface modeling hybrid methods

Although the MPM has proven effective for modeling a wide range of large deformations, various solution variants have been proposed and developed in conjunction with other numerical discretization schemes (e.g. FEM (Higo et al., 2010; Zhu et al., 2022), DEM (Wang et al., 2022a; Liang et al., 2023a; Li et al., 2024), SPH (Raymond et al., 2016), computational fluid dynamics (CFD) (Tran et al., 2024), peridynamics (PD) (Zeng et al., 2022), molecular dynamics (MD) (Wang et al., 2023b), and discontinuous deformation analysis (DDA) (Hashimoto et al., 2022)), driven by considerations of efficiency, accuracy, and applicability. In this section, two hybrid methods, the MPM-DEM and the MPM-FEM, are described in detail.

As a hybrid continuum-discrete approach, the MPM-DEM offers greater robustness and efficiency for modeling solid-granular interactions compared to pure continuum or discrete methods. The key to MPM-DEM coupling is accurate detection and calculation of the contact force between the MPs and DEM particles. Liu et al. (2018) proposed a method in which MPs are attached to DEM particles, and both contact detection and contact forces are performed using a pure MPM contact algorithm (Bardenhagen et al., 2000). However, this coupling method still inevitably suffers from a dependency on a grid system for contact calculations within pure MPM schemes. Jiang et al. (2020) proposed a different approach for contact computation. This method uses the Euclidean distance between particle centroids and positions to detect contact relationships and directly calculates contact forces based on the DEM contact model. The MPM-DEM formulation was further enhanced by introducing a barrier method that rigorously couples MPs and discrete elements, preventing any interpenetration under high impact loads (Jiang et al., 2022). This method shows great promise for accommodating highly complex solid-granular interactions.

The domain decomposition-based MPM-FEM hybrid scheme has been extensively studied over the last decade for various application scenarios involving multi-material simulations or strongly heterogeneous deformations. In the coupling MPM-FEM system, FEM vertices are commonly treated as MPM particles and embedded into the MPM grid (Lian et al., 2011), ensuring that grid-based MPM contact characteristics are naturally inherited for handling multi-material interactions. However, the grid-based MPM-FEM coupling strategy also inherits the premature contact issue and requires that the FE boundary element size be close to the MPM background size to ensure contact accuracy. Accordingly, Cheon and Kim (2018) introduced distributed interaction nodes on the contact faces of an FE mesh to increase the resolution and computational efficiency of contact calculations. They also adopted a weighted distance method to eliminate early contact nodes and improve detection precision. Furthermore, most MPM-FEM coupling frameworks have been designed for explicit time integration, which poses challenges when the associated inequality constraints need to be enforced simultaneously by solving the nonlinear system of equations in implicit time integration. In recent years, Li et al. (2022a) proposed a novel monolithic approach that couples the MPM with the FEM through barrier energy-based particle-mesh frictional contact, employing a variational time-stepping formulation. The proposed coupling scheme can be viewed as a contact method. It imposes separable frictional motion boundaries when all nodal displacements within the FEM domain are subjected to Dirichlet boundary conditions.

Overall, the application of the MPM in modeling geo-interfaces, while challenging, can effectively enhance the accuracy and efficiency of simulations by employing appropriate methodologies and strategies. The different MPM approaches for modeling material interfaces, state interfaces, and motion interfaces are discussed in the following sections.

4. Modeling of the material interface

Material interfaces refer to the contact surfaces between media with distinct physical and mechanical properties (Zhu, 2023), such as the interfaces between rock and soil, soil and concrete, or concrete and steel. Failures at these interfaces often result from load transfer and stress concentrations due to disparities in the modulus (Zhao et al., 2022a). Numerical methods provide a powerful approach for investigating the mechanical behavior of material interfaces (Nayroles et al., 1992). Various numerical techniques have emerged and can be classified into three primary categories: continuum elements, contact approaches, and interface elements (Zhang and Zhang, 2009; Saberi et al., 2018).

4.1. *Continuum element*

The first type of numerical technique for simulating the material interface involves continuum elements with standard constitutive laws. This method applies the constitutive model of soil directly to the soil-structure interface (Reissner, 1936; Zdravković, 1999; Zhang et al., 2023c). Nevertheless, by treating the soil as an idealized material, the behavior of the continuum element can be oversimplified (Gazetas and Tassoulas, 1987; Zhang and Zhang, 2009). Consequently, the stress-strain relationship of the soil-structure interface must be thoroughly evaluated when the continuum element is employed, particularly in situations with significant deformation (Luco, 1998). In the MPM, the default contact between different bodies is considered a nonslip contact, given that their velocities belong to the same vector field (Beuth et al., 2011; Talmon et al., 2019; Ceccato et al., 2020; Martinelli and Galavi, 2021, 2022; Zhao et al., 2021; Galavi and Martinelli, 2024). In other words, to prevent relative motion, friction across the contact area can be considered to approach infinity. This characteristic makes the MPM well suited for simulating non-slipping adhesive contacts, such as the bearing capacity of rough strip footings (Gao et al., 2023; Xie et al., 2023), rock layer compression and folding (Lenardic et al., 2000), and the collapse of sand columns (Shi et al., 2018). Conversely, for scenarios involving slipping or separation, the use of contact algorithms or interface elements becomes necessary.

4.2. *Contact approach*

The second type of numerical technique for modeling material interfaces is the contact approach, which is based on contact mechanics (Zhang and Zhang, 2009). This method establishes contact equations for stress transfer by directly defining the interfacial mechanical transfer laws between different media. These equations are subsequently resolved via specialized contact algorithms. Many algorithms, including Lagrange methods and penalty function methods, have been developed to analyze the behaviors of material interfaces (Ma et al., 2014; Fern et al., 2019; de Vaucorbeil et al., 2020). In the MPM, contact algorithms are commonly employed to simulate the material interface (Al-Kafaji, 2013; Chen et al., 2023; Zhao et al., 2023b; Cuomo et al., 2024; Xie et al., 2024b). For example, the friction contact algorithm is widely used in soil-structure interactions (Bardenhagen et al., 2000; Bardenhagen, 2001; Yang and Qiu, 2020; Li et al., 2023b; Tu et al., 2023). As illustrated in Fig. 7, the initial prediction of nodal velocities occurs in the Lagrangian phase. Thereafter, the friction contact algorithm is utilized to compute the corrected nodal velocities and accelerations. These updated nodal accelerations are then employed to calculate the velocities of the MPs, further updating their positions, strains, and stresses in the convective phase (Coetzee et al., 2005; Zhu et al., 2023).

Moreover, conventional friction contact algorithms (Sulsky et al., 1994; York et al., 2000; Bardenhagen et al., 2000) have been enhanced with a novel approach termed ‘geo-contact’ (Ma et al., 2014). This algorithm configures two Eulerian meshes for the soil and the structures, fa-

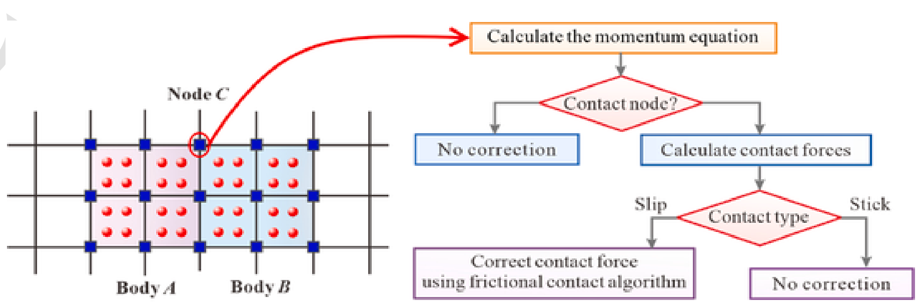

Fig. 7. Flow chart of the friction contact algorithm.

cilitating a multi-valued nodal velocity field. Furthermore, within the standard multi-field velocity adjustments between the soil and rigid structures, a penalty function is introduced to adjust the relative velocities, thereby ensuring a relatively stable reaction force. Using the 'geo-contact' method, the impact forces that landslides exert on structures can be accurately predicted (Dong et al., 2017a, 2020b). In summary, the contact approach in the MPM can handle complex contact issues such as interactions between different material interfaces. It is particularly effective for addressing challenges associated with large deformations. However, the computational cost can significantly increase when a large number of MPs are involved. Under extreme conditions, such as very high-speed collisions or interactions over very small contact areas, MPM contact algorithms may suffer from numerical instabilities. These can manifest as penetration or oscillatory problems.

4.3. Interface element

The third type of numerical technique used in material interface analysis is the interface element. This method has garnered attention for its ability to accurately model the mechanical behavior of material interfaces, particularly given the thinness of the interface and the substantial constraints imposed by the surrounding structures (Zhang and Zhang, 2009; Dhadse et al., 2021, 2023). Both the type of element chosen and its corresponding constitutive model are pivotal factors influencing the accuracy of the interface element in numerical simulations. Interface elements can be broadly classified into two categories: zero-thickness elements, as introduced by Goodman et al. (1968), and thin-layer elements, as proposed by Desai et al. (1984). Further elaborations are presented in the following subsections.

4.3.1. Zero-thickness element

To address a jointed rock mass, Goodman et al. (1968) proposed a specialized element known as the zero-thickness or Goodman contact element. This element has subsequently been further developed and extensively employed in soil-structure contact problems (Bojanowski, 2014; Wang et al., 2015, 2022b; Liao et al., 2020). As depicted in Fig. 8, numerous tiny orthogonal springs are spread across the contact surface between the two materials (Goodman et al., 1968). The zero-thickness element accurately models displacement discontinuities at the contact interface, thereby enabling an effective representation of phenomena such as dislocation slippage, expansion of the contact area, and nonlinearities in contact surface deformation. Nonetheless, using the Goodman contact element requires consistent upper and lower meshes, which adds complexity to the computations (Desai et al., 1984). Additionally, because the stiffness of the interface greatly exceeds that of the corresponding soil part, this may lead to potentially inaccurate predictions of normal stresses. As noted by Pande and Sharma (1979), Day and Potts (1994), and Zdravković (1999), the zero-thickness element generally provides a conservative estimate of the soil-structure interface.

4.3.2. Thin-layer element

Given the challenges associated with the zero-thickness interface element, Desai et al. (1984) introduced a thin-layer element method as a viable alternative. Notably, the thin-layer element can revert to the Goodman contact element if the thickness of the interface is set to zero. Desai et al. (1984) reported that the interface between the soil and structure is thick. This interface exhibits behavior that differs from that of adjacent soils. Several studies offer suggestions for selecting the thickness, specifically within the range of (0.01–0.1)D, where D represents the average size of the adjacent element (Uesugi et al., 1988; Frost et al., 2002, 2004; Hu and Pu, 2004; DeJong et al., 2006). The thin-layer element can transmit force and represent contact behaviors, including bonding, slipping, gapping, and reclosing, as shown in Fig. 9. This element has received increasing attention for its accurate modeling of the normal and tangential stress-strain relationships of the interface (Zhang and Zhang, 2009).

In the MPM, interface elements can also simulate large deformations at material interfaces. Vermeer et al. (2009) and Wang et al. (2017) used interface elements to investigate penetration problems, such as screwpile installation. However, using interface elements in MPM remains challenging due to the non-coincidence of the grid domain and the material domain. Consequently, contact approaches are still widely used in MPM to model sliding contacts between different contacting bodies. Nonetheless, interface elements can enhance contact simulations in complex scenarios. This is especially useful in geotechnical structure joints, which require detailed consideration of interface interactions. Therefore, future research could focus on integrating more interface elements into the MPM framework to better simulate challenges associated with large deformations at material interfaces.

5. Modeling of state interface

The state interface denotes the interface where the state parameters involving moisture, stress, or temperature in geo-materials exhibit sudden transitions (Zhu, 2023). Many studies have demonstrated that factors such as rainfall infiltration, groundwater level fluctuations, and pore pressure are the main causes of landslides (Andersen and Andersen, 2010; Liu et al., 2019; Yerro et al., 2019), levee failures (Zabala and Alonso, 2011), and water–soil gushing in shield tunnels (Xie et al., 2022). Owing to its algorithmic similarities with the well-studied FEM, the MPM is highly effective at capturing hydro-mechanical behavior in large deformation analyses, particularly with the use of appropriate soil constitutive models. Currently, the MPM includes formulations such as two-phase single-point, two-phase double-point, and three-phase single-point methods for soil-water coupling. The details of various MPM numerical approaches are illustrated in Fig. 10 and are further elaborated in the following subsections.

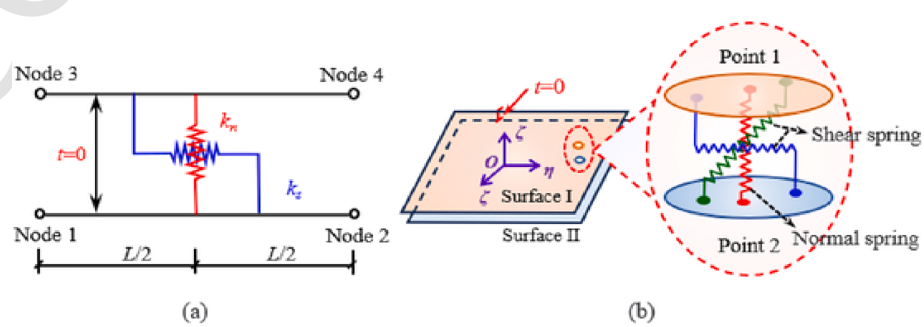

Fig. 8. (a) 2D Goodman contact element model and (b) 3D Goodman contact element model.

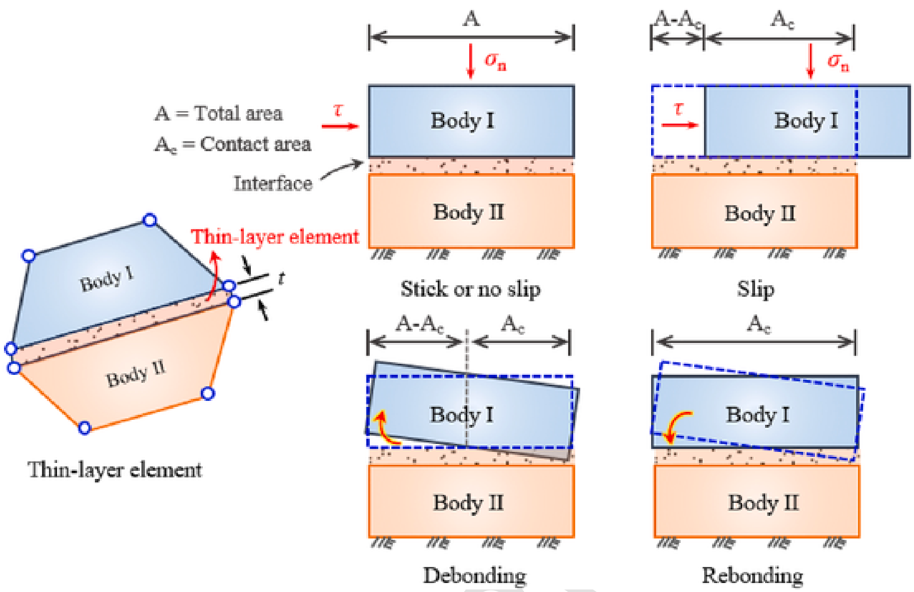

Fig. 9. Thin-layer element and deformation modes at the interface (adapted from Desai et al. (1984)).

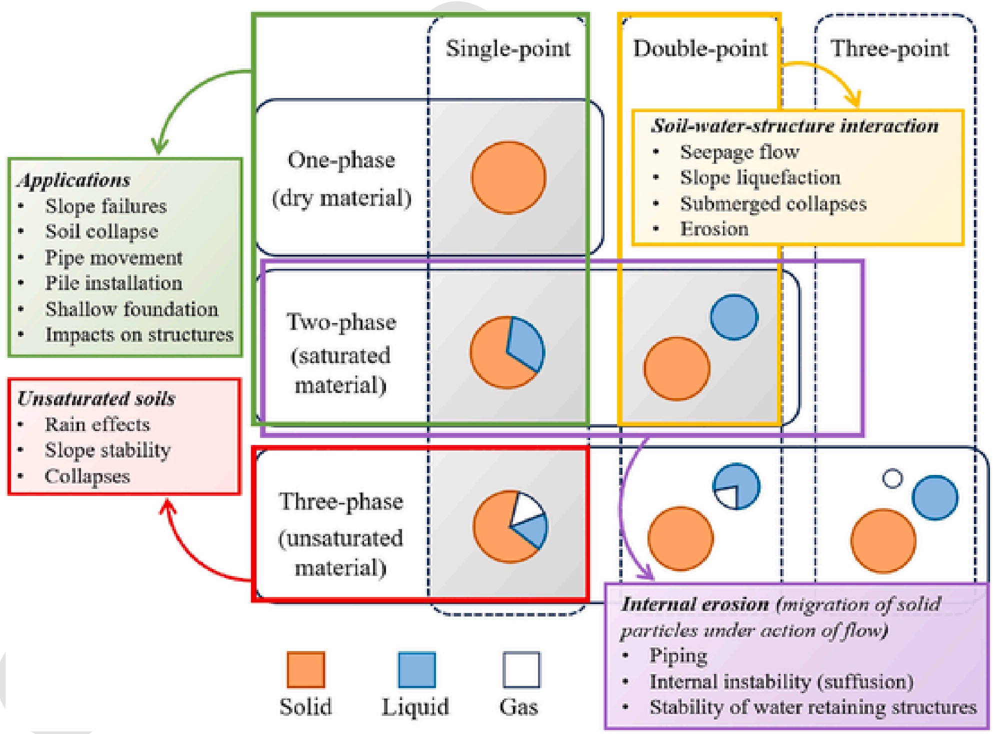

Fig. 10. Scheme of different MPM numerical approaches depending on the number of phases and the number of MP sets (adapted from Yerro et al. (2015)).

5.1. Single-point approach

Recent developments in the MPM for studying multi-phase problems can be categorized into two approaches: using either one or two layers of MPs to describe the response of distinct phases (Jassim et al., 2013; Soga et al., 2016; Zheng et al., 2024). In the two-phase single-point approach depicted in Fig. 11, the MPs contain all the soil and water phase information. Soil particles are described via material coordinates in the Lagrangian formulation, whereas pore water is modeled via the Eulerian formulation with spatial coordinates (Chen et al., 2017; Conte et al., 2020; Shi et al., 2020). However, it is important to note that this approach may not effectively address high-frequency issues involving rapid deformations (Soga et al., 2016; de Vaucorbeil et al., 2020).

Considering gas in unsaturated soils, Yerro et al. (2015) presented a three-phase single-point MPM formulation, as shown in Fig. 12. This approach derives its governing equations from the balance of momentum and mass of the solid, liquid, and gas phases, taking into consideration a non-zero gas pressure. In addition to the three-phase single-point approach, the two-phase single-point approach with suction is also em-

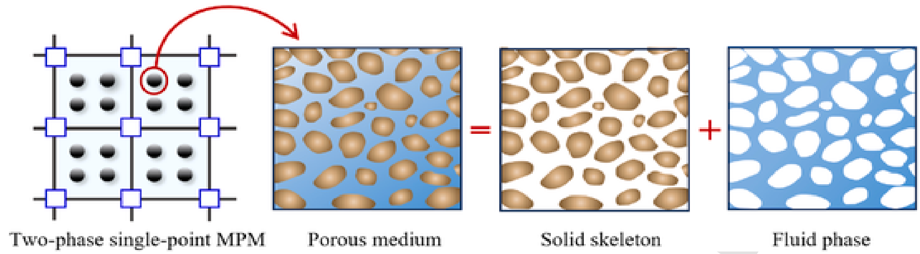

Fig. 11. Schematic diagram of the two-phase single-point MPM approach (adapted from Soga et al. (2016)).

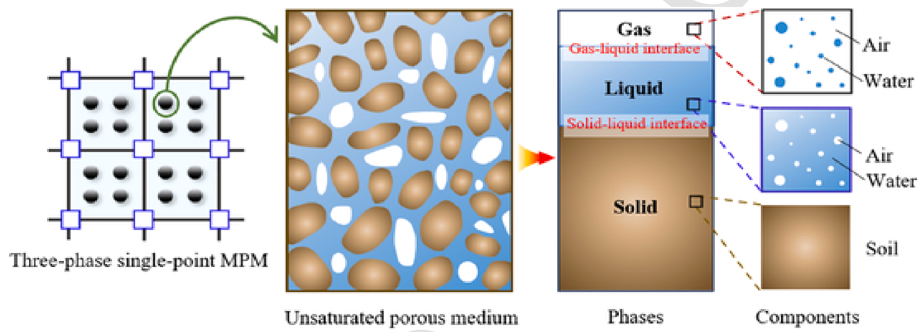

Fig. 12. Schematic diagram of the three-phase single-point MPM approach (adapted from Yerro et al. (2015)).

ployed to simulate the capabilities of unsaturated soils (Bandara et al., 2016; Martinelli et al., 2020; Cuomo et al., 2021c).

5.2. Double-point approach

As illustrated in Fig. 13, the coupled MPM can also employ two sets of Lagrangian MPs to account for solid and liquid materials (Wieckowski, 2013; Bandara and Soga, 2015; Martinelli, 2016; Liu et al., 2017; Tran and Sołowski, 2019; Monzer et al., 2023). Employing two layers of MPs, one each for the solid and liquid phases, effectively ensures mass conservation for both phases and accurately captures their interactions (Soga et al., 2016; Ceccato et al., 2020). Using two MP layers offers significant advantages in modeling soil–water interaction problems, such as submarine landslides, dike erosion, and surge processes (Martinelli et al., 2017a, 2017b; Liang et al., 2020; Du et al., 2021, 2023; Monzer et al., 2023). However, using two layers of MPs significantly increases computational expenses and leads to numerical instabilities, thereby restricting its practical application (Soga et al., 2016; Ceccato et al., 2018a; Fern et al., 2019; Zheng et al., 2024). Notably, neither the coupled MPM for the three-phase double-point approach nor the three-phase three-point approach has been developed. This is because implementing two or three sets of MPs involves substantial computational costs (Yerro et al., 2015; Soga et al., 2016; Sołowski et al., 2021). For further details, the interested reader can find insight-

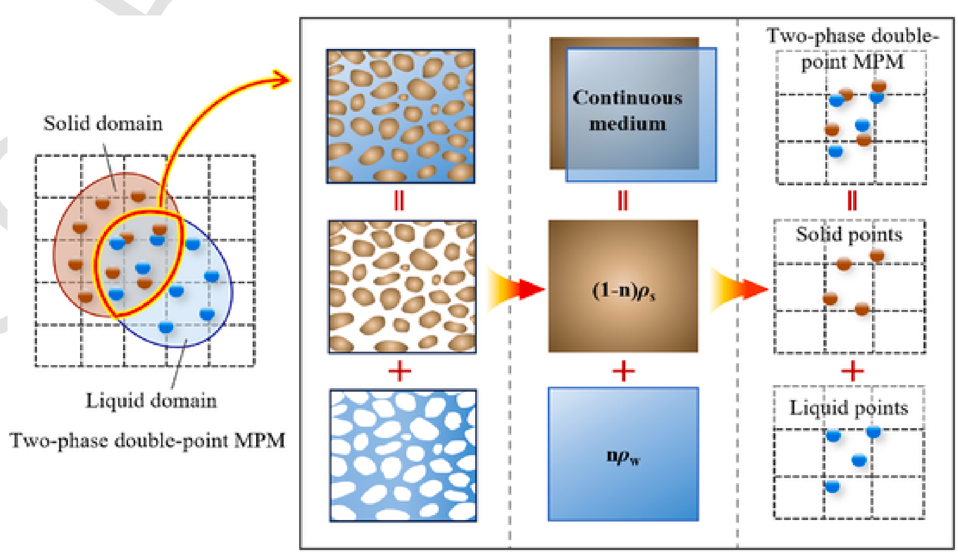

Fig. 13. Schematic diagram of the two-phase double-point MPM approach (adapted from Soga et al. (2016)).

ful comparisons between these multi-phase MPM formulations in literature reviews (Yerro et al., 2022; Ceccato et al., 2024; Zheng et al., 2024).

6. Modeling of the motion interface

The motion interface is where macroscopic deformation and failure occur within rock and soil masses or at the interface between the soil and adjoining structures (Zhu, 2023). These interfaces often manifest as shear zones or slip surfaces. As previously mentioned, the MPs in the MPM can cross the background mesh. Therefore, it is crucial to track MPs at each time step before computing the mapping functions to ensure accuracy (Bisht et al., 2021; Feng and Xu, 2021; Baumgarten and Kamrin, 2023). As shown in Fig. 14, maintaining computational accuracy is essential when simulating penetration problems such as pile driving and shallow foundation issues. Mesh refinement near the soil-structure interface, where variations in the solution can occur rapidly, has proven effective (Chen et al., 2019; Wang et al., 2021b).

To maintain a consistently fine mesh around the structure, the moving mesh approach is employed (Al-Kafaji, 2013; Phuong et al., 2016; Ceccato et al., 2016, 2020). The computational domain is divided into moving and compressed mesh zones (as depicted in Fig. 15). During the penetration process, the moving mesh zone moves at the same velocity as the structure without requiring mapping between the MPs and nodes (Ceccato et al., 2016; Martinelli and Galavi, 2021, 2022; Yost et al., 2022, 2023; Galavi and Martinelli, 2024). Unlike the fixed shape of the elements in the moving mesh zone, the grid in the compressed mesh zone undergoes deformation. Compression is distributed linearly with depth, resulting in nodes at the top of the compression zone displacing identically to the structure, whereas nodes at the bottom remain stationary (Beuth et al., 2011; Bisht et al., 2021). A key benefit of the moving mesh approach is its ability to maintain the soil-structure interface without requiring reidentification, thus avoiding inaccuracies (Soga et al., 2016; Ceccato and Simonini, 2017). Notably, some studies on soil–structure interactions have utilized only a moving mesh, eliminating the need for a compressible mesh (Talmon et al., 2019; Zwanenburg et al., 2023).

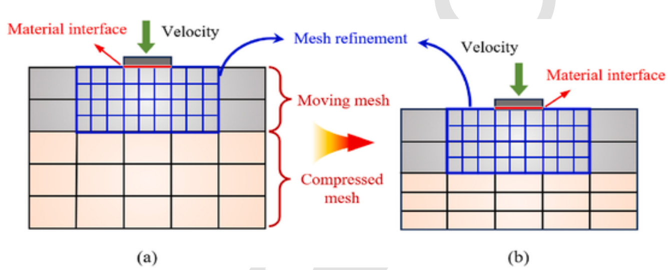

Fig. 14. Mesh refinement and moving mesh: (a) Before penetration, and (b) After penetration.

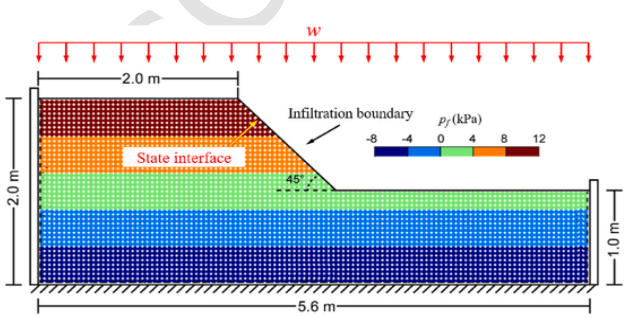

Fig. 15. MPM model of rainfall-induced slope failure (reproduced from Wang et al. (2023a) with permission from Elsevier).

Furthermore, the use of the MPM to simulate motion interfaces presents significant challenges due to the non-coincidence of the mesh and material domains, particularly when boundary conditions are imposed. For fixed rigid boundaries, such as landslides on bedrock, unstructured triangular meshes prove effective in addressing these complexities (Fern et al., 2019). Additionally, for moving contact interfaces, contact distance criteria can also be integrated to identify these interfaces (Ma et al., 2014; Nakamura et al., 2021; Chen et al., 2023; Liang et al., 2023a). These methods offer effective solutions for simulating motion interfaces in the MPM.

7. Geo-interface analysis using the MPM

MPM analysis plays a crucial role in investigating large deformation problems at geo-interfaces and their implications for engineering structures. This section explores the utilization of the MPM in simulating such deformations, including slope collapse and landslide dynamics, soil-structure interactions, and failure mechanisms of human-induced geologic hazards. These applications reveal complex behaviors at various geo-interfaces. Through a series of case studies, this section aims to highlight the effectiveness of the MPM in simulating the evolution of geo-interfaces, providing insights crucial for disaster prevention and mitigation in geotechnical engineering.

7.1. Slope collapse and landslide dynamics analysis

Slope collapse and landslides triggered by rainfall and earthquakes pose significant threats to human safety, ecosystems, and the security of geotechnical structures (Saito et al., 2014; Bandara et al., 2016; Martinelli et al., 2020; Cuomo et al., 2021c). Owing to climate extremes and earthquakes, the frequency of slope collapse and landslides has increased (Kirschbaum et al., 2010; Zhao et al., 2023b). Understanding the mechanisms of slope failure and conducting quantitative risk assessments for landslides have become crucial. Therefore, employing advanced numerical methods is essential for accurately modeling the evolution of large deformations at geo-interfaces.

7.1.1. Rainfall-induced slope collapse

To investigate the influence of different rainfall intensities on slope failure processes, Wang et al. (2023a) simulated rainfall-induced slope failure using the single-point multi-phase MPM. The Drucker-Prager (DP) constitutive model with suction-dependent reduction (Yerro et al., 2015) was introduced to capture the evolution of the state interface and motion interface. Furthermore, GPU acceleration techniques have been used to increase simulation efficiency (Dong et al., 2015). The top surface of the slope was subjected to a rainfall infiltration boundary condition, with a prescribed rainfall intensity represented by w (where w = 0 mm/h for non-rainfall conditions). The model was discretized using 6500 MPs, with a grid size of 0.1 m and 8 MPs per element. Initially, the stress and suction fields reached equilibrium under gravity. The top elements of the slope registered a suction (p_f) of 12 kPa, as illustrated in Fig. 15.

The prescribed rainfall intensity w was subsequently increased to initiate the rainfall simulation process. Throughout the simulation, the evolution of the state and motion interfaces becomes apparent with changes in rainfall intensity. As depicted in Fig. 16, the migration of the state interface reduces the effective stress within the soil, weakening the stability of the slope. When the rainfall intensity is low, the motion interface progresses deeply and then extends to the slope toe, leading to significant bulk failure of the slope. Conversely, with high rainfall intensities, the motion interface is more likely to occur near the shallow slope surface. These observations confirm that variations in rainfall intensity directly affect the evolution of geo-interfaces, thereby influenc-

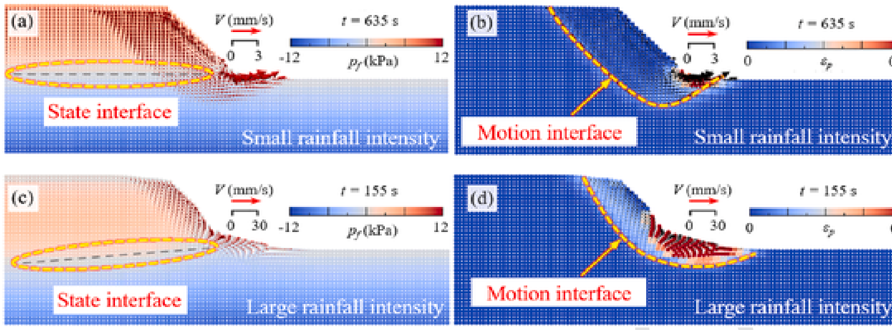

Fig. 16. Different failure patterns induced with different rainfall intensities (reproduced from Wang et al. (2023a) with permission from Elsevier).

ing the stability and failure behavior of slopes. Therefore, understanding the relationship between rainfall intensity and geo-interfaces is crucial for the effective prediction and management of slope failure.

7.1.2. Earthquake-induced landslides

In the MPM, dynamic boundary conditions can be applied to simulate the complex geo-interface transformation process. To understand the mechanisms of failure initiation, the runout process, and the affected areas of the Daguangbao landslide, Fernández et al. (2023) developed the MPM-PUCRio code (Fernández et al., 2020) to model this earthquake-induced landslide in three dimensions. As depicted in Fig. 17, the model was constructed via 3D elevation data from the landslide region. The simulation was divided into an initial geostatic stage and a subsequent dynamic failure stage. First, the elastic and elastoplastic behavior of the material was considered in the quasi-static analysis. Then, the seismic load was applied to the bottom boundary particles, while the model lateral sides were imposed with lateral and non-reflecting boundary conditions. This work modified the equation of motion within the MPM framework to include a viscous force term, enhancing the non-reflecting boundary conditions that dissipate seismic wave energy. Frictional contact algorithms model the material interface between the soil and base rock. The simulation parameters were based on laboratory tests reported by He et al. (2019). An adjustment analysis was used to determine the friction angle at the interface between the landslide body and its base, ensuring equilibrium and alignment with observed post-landslide topographical changes. The strain-softening Mohr-Coulomb (SSMC) model was introduced to capture the evolution of the motion interface. The computational mesh, with a side length of 50 m, comprises 8 MPs, i.e., 2 MPs in each coordinate direction.

Fig. 18 illustrates the motion interface evolution process of the landslide. The development of the motion interface begins with the elastoplastic response of the soil. As seismic loads persisted, the mo-

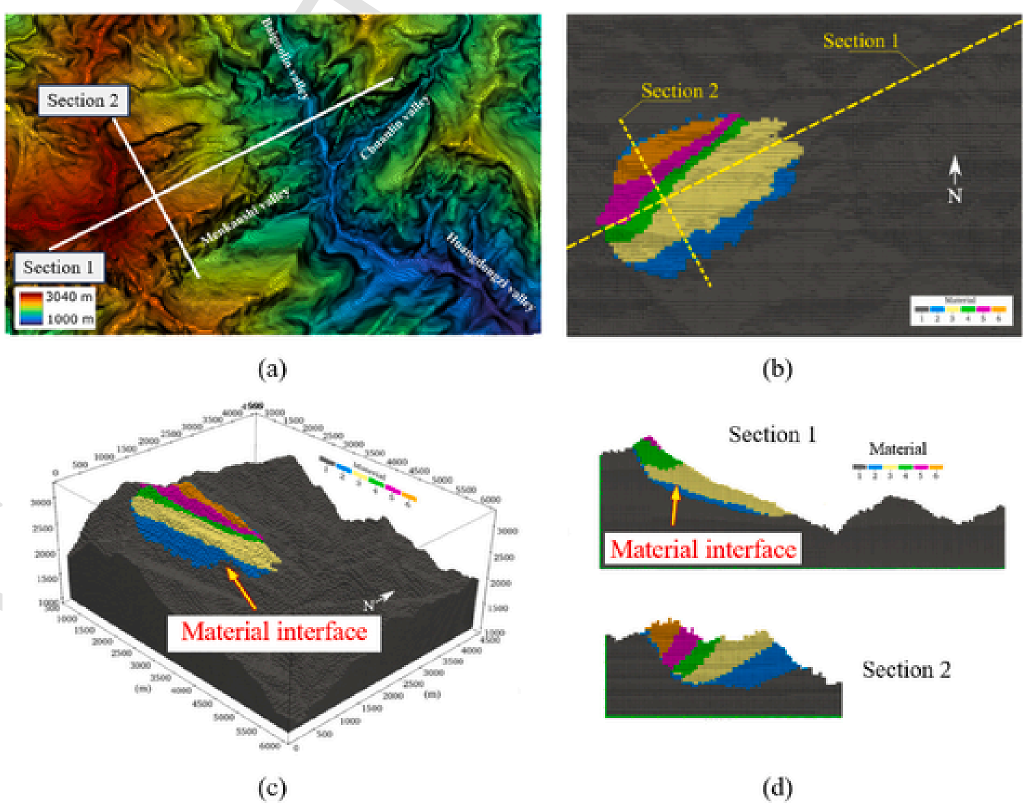

Fig. 17. Topography of the landslide and 3D MPM model: (a) topography of the landslide, (b) numerical model, (c) 3D view of the MPM model, and (d) sectional view of the MPM model (reproduced from Fernández et al. (2023) with permission from Springer).

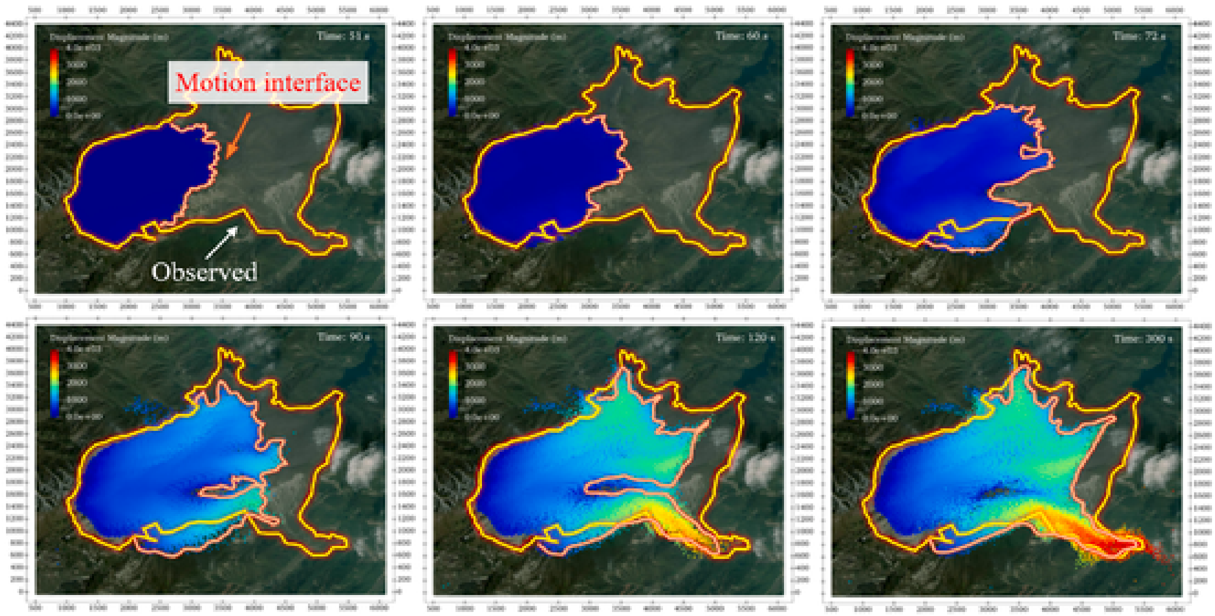

Fig. 18. Runout evolution of landslides (reproduced from Fernández et al. (2023) with permission from Springer).

tion interface expanded across the slope surface and into deeper layers. The interface reached full activity when the entire landslide mass was mobilized, leading to significant displacement and the formation of a landslide dam. The total affected area, as determined by the MPM, aligned closely with the observed data, with an error of approximately 0.4 %. Additionally, the shape of the affected area remained consistent, with a maximum width error of 11 % and a length error of 9 %. These results demonstrate that the MPM is an effective tool for simulating large-scale landslides and capturing the complex evolution of three-dimensional large deformations of geo-interfaces. Furthermore, Shi et al. (2019) used the MPM to study the motion interface of the Shenzhen landfill landslide, further underscoring the critical role of the motion interface in the dynamic evolution of landslides.

7.2. Analysis of the soil-structure interaction

In the field of geotechnical engineering, analyzing soil-structure interactions is crucial for assessing potential soil failure modes and the safety of geotechnical structures. The complex behaviors at geo-interfaces include the evolution of motion interfaces in the soil, the migration of state interfaces, and variations in stress across the material interfaces of structures. Therefore, it is essential to employ advanced numerical methods to capture the detailed processes of evolution at these geo-interfaces.

7.2.1. Uplift failure of buried pipes

Uplift failures of underground pipelines typically arise from natural hazards (O'Rourke, 2010; Sim et al., 2012). Furthermore, human activities such as aquifer over-pumping (Wols and van Thienen, 2014), urban tunneling (Wang et al., 2011), and deep excavation contribute to these failures. These failures lead to complex changes in the motion interfaces of the pipe-soil system. Zhang et al. (2023a) employed the open-source code MPM3D-F90 (Zhang et al., 2016b) to simulate the uplift failure of buried pipes. The non-associative Mohr-Coulomb (MC) model and SSMC model were utilized to capture the behavior of the motion interfaces. Fig. 19 shows the geometric characteristics and initial MPs of the MPM model. The pipe was modeled as a rigid cylinder with an outer diameter D (the green zone in Fig. 19).

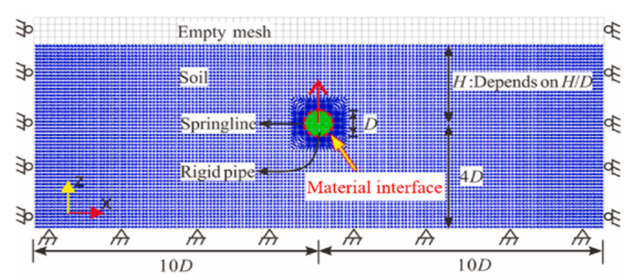

Fig. 19. MPM numerical model (reproduced from Zhang et al. (2023a) with permission from Elsevier).

Fig. 20 shows the evolution of the motion interface for $H/D = 3$, which is characterized by the formation and transformation of shear bands. Initially, shear bands form with specific angles reflecting the peak soil dilation angle. As uplift progresses, these shear bands may rotate and decrease in inclination, indicating a reduction in soil resistance, particularly under shallow conditions. The motion interfaces captured by the SSMC model are influenced primarily by three factors: the soil wedge size, the shear resistance along the shear bands, and the flow-around mechanism. However, the shape of the motion interfaces captured by the MC model remains essentially constant because of the use of a constant effective dilation angle. In addition to analyzing pipeline uplift failure, the MPM also assesses motion interfaces during downward and lateral pipe movements (Zhang et al., 2023a; Xie et al., 2024b). In studying pipeline vertical downward relative offsets, Zhang et al. (2023a) utilized the J_2 deformation-type soil constitutive model to investigate pipe-soil interactions and reported that this advanced constitutive model can better capture motion interfaces, which are affected by nonlinear stress-strain relationships and state-dependent dilatancy (Fu et al., 2024). This is critical for understanding the dynamic interactions at geo-interfaces and their implications for pipeline integrity and safety.

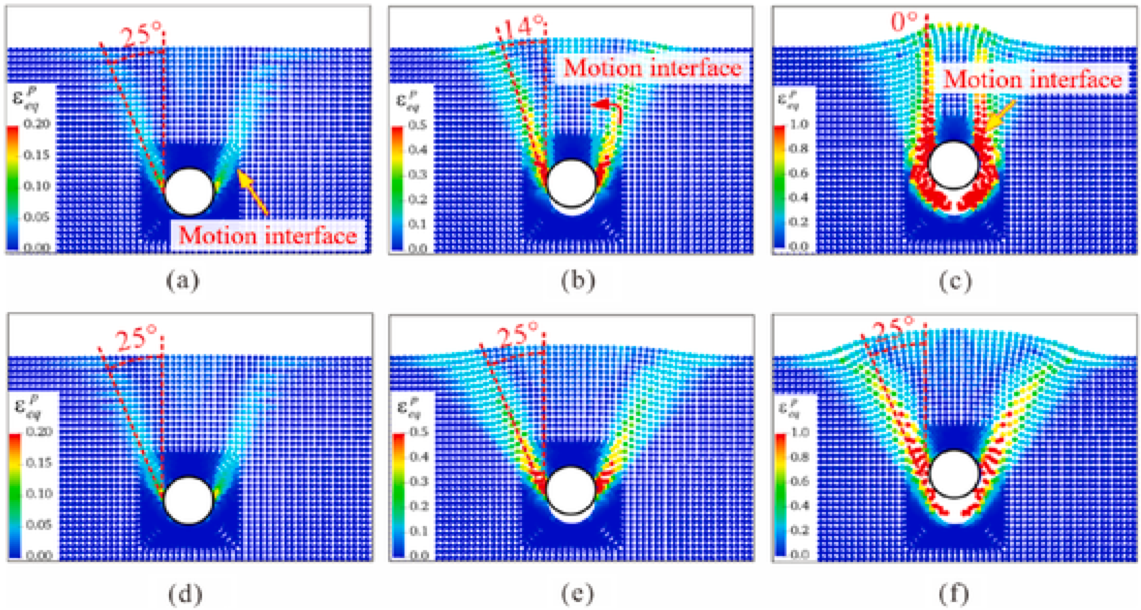

Fig. 20. Shear band formation: (a–c) SSMC model and (d–f) MC model (reproduced from Zhang et al. (2023a) with permission from Elsevier).

7.2.2. Impact forces on pipelines caused by submarine landslides

Submarine landslides are among the most destructive submarine geohazards, transporting heavy sediments at speeds of up to 20 m/s (Jakob et al., 2012). These landslides can significantly affect the integrity and functionality of subsea pipelines, which are commonly used to transport oil and gas, as well as to protect subsea cables. Therefore, understanding the stress changes at the material interfaces between the soil and the structure is crucial for ensuring the safety of these structures. Dong et al. (2017a) simulated the impact of a submarine landslide on a fixed subsea pipeline using the MPM-GeoFluidFlow program, which is driven by multiple-GPU hardware (Dong et al., 2015). As depicted in Fig. 21, a rectangular soil block with height H and length L is given an initial horizontal velocity v over a smooth rigid base. A partially buried pipe with a diameter D is positioned directly in front of this sliding mass. The material interface between the smooth pipe and the soil is governed by the 'geo-contact' algorithm (Ma et al., 2014). The sliding material was modeled using a simple total stress von Mises failure envelope, with the rate-dependent shear strength derived from the Herschel-Bulkley (H-B) rheological model (Locat and Lee, 2002). Each element contains 16 MPs to ensure higher accuracy in addressing the dynamic problem.

A comprehensive analysis was conducted on 650 cases to investigate various scenarios regarding the shape and characteristics of the sliding material. The use of impact coefficients, which quantify the effect of dynamic loads transmitted through material interfaces, is particularly important. These coefficients provide a clear measure of how variations in the velocity and mass of sliding debris influence the stresses experienced by pipelines. The normalized impact pressures obtained via the MPM are expressed as $p/(\rho v^2)$:

$$\frac{p}{\rho v^2} = 0.5C_D + N_c\frac{1}{R_e} + C_\gamma\frac{(\rho-\rho_W)}{\rho}\frac{1}{F_r^2} \tag{1}$$

where C_D is the drag coefficient, N_c is the bearing capacity factor, R_e is the Reynolds number, C_γ refers to the static coefficient, and F_r is the Froude number. Regression analysis was employed to fit the coefficients of the impact forces obtained by the MPM, as shown in Fig. 22. This quantification is crucial for the design of structures. Through detailed analyses of the material interface, the MPM not only facilitates an understanding of the current structural responses but also aids in predicting future behaviors under similar or more severe conditions.

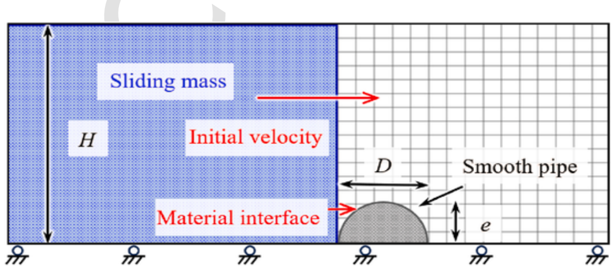

Fig. 21. MPM model of a submarine landslide across a pipeline (adapted from Dong et al. (2017a)).

7.2.3. Water-soil gushing in tunnels

Water-soil gushing accidents in shield tunnels have been intermittently observed (Cheng et al., 2020; Huang et al., 2020; Tan and Lu, 2017; Zhang et al., 2021). This phenomenon typically occurs at material interfaces, such as joints and holes in prefabricated segment linings, posing significant risks to the integrity of tunnels and the stability of the surrounding soil. Therefore, understanding the evolution of motion interfaces and the migration of state interfaces during water-soil gushing events is crucial. Xie et al. (2022) utilized the open-source code Anura3D (2020) to model water-soil gushing in tunnels. Fig. 23 shows a schematic diagram of the MPM model and its boundary conditions. The model employs a two-phase single-point approach and the MC model to capture the behaviors of geo-interfaces. A contact algorithm was applied to model the tunnel-soil material interface. With respect to the mesh configuration, the computation mesh primarily consisted of triangular elements, each 0.75 m in size and initially containing 3 MPs.

Fig. 24 presents the behavior of geo-interfaces during gushing at the tunnel crown. Initially, when water-soil begins to intrude into the tunnel through openings or joints, it disrupts the original equilibrium, forming motion interfaces. These interfaces were initially localized but became more pronounced as the water-soil gushing process developed. As the system approaches a new equilibrium, the expansion of motion

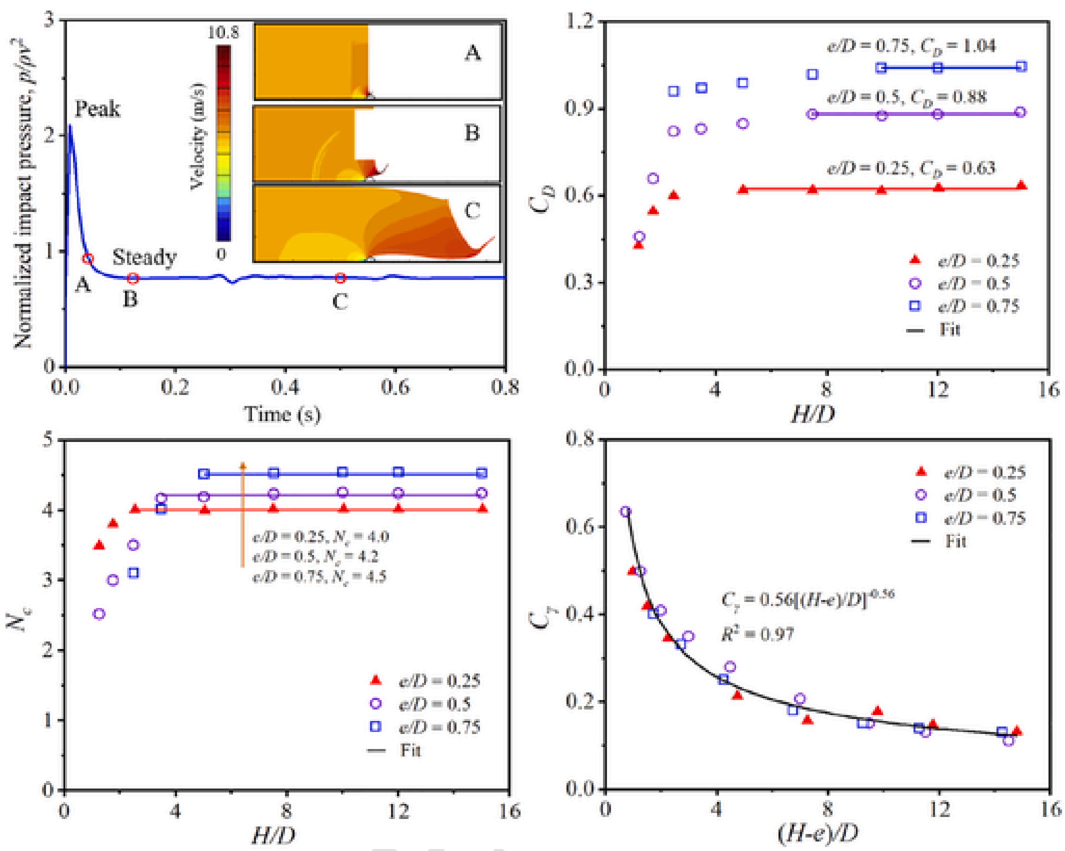

Fig. 22. Curves of impact pressure and fitted functions of C_D, N_c, and C_γ (adapted from Dong et al. (2017a) with permission from Elsevier).

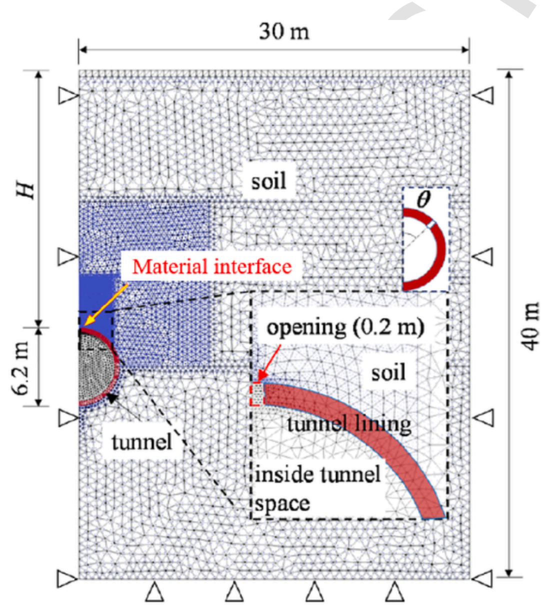

Fig. 23. Typical model configuration of the MPM numerical model for water–soil gushing (reproduced from Xie et al. (2022) with permission from Elsevier).

interfaces stabilizes. The area surrounding the tunnel was categorized into three distinct zones according to the motion interface: the flow zone, the disturbed zone, and the stationary zone. Each zone reflected varying degrees of soil response to the gushing. Changes in the state interface were evidenced by variations in the pore water pressure. Initially, the pore pressure was at a hydrostatic level, but it rapidly decreased near the opening as the gush began. This decrease led to pore pressure dissipation, causing significant changes in the state interface. The pore pressure eventually stabilized at a new equilibrium, indicative of a consolidation phase. The observed similarities in the shapes of the state and motion interfaces suggested dynamic interactions among these geo-interfaces. Therefore, it is essential to implement comprehensive measures, such as monitoring and reinforcement, to mitigate hazards associated with these interfaces in geotechnical engineering.

In addition to the previously discussed examples, the MPM has been applied to simulate soil-water-structure interactions during cone penetration tests (CPTs). These studies effectively highlight how the MPM captures the dynamic behavior of geo-interfaces, detailing the migration of the state interface and evolution of the motion interface during penetration (Ceccato et al., 2016; Ceccato and Simonini, 2017; Yost et al., 2022). Additionally, the MPM has been utilized to model the interactions at the material interface during the pile installation process (Phuong et al., 2016; Fu et al., 2024; Galavi and Martinelli, 2024). The insights gained from these MPM applications highlight their efficacy in addressing complex geotechnical problems and deepening our understanding of geo-interface behaviors.

7.3. Human-induced geologic hazards

Human activities have triggered numerous geologic hazards that pose significant threats to human life and property. Among these fissures, pumping-induced earth fissures have attracted particular attention from researchers. Numerous studies have shown that earth fissures typically occur at the periphery of a basin (Budhu, 2008), atop a bedrock ridge (Wang et al., 2016d), or near a buried fault (Peng et al.,

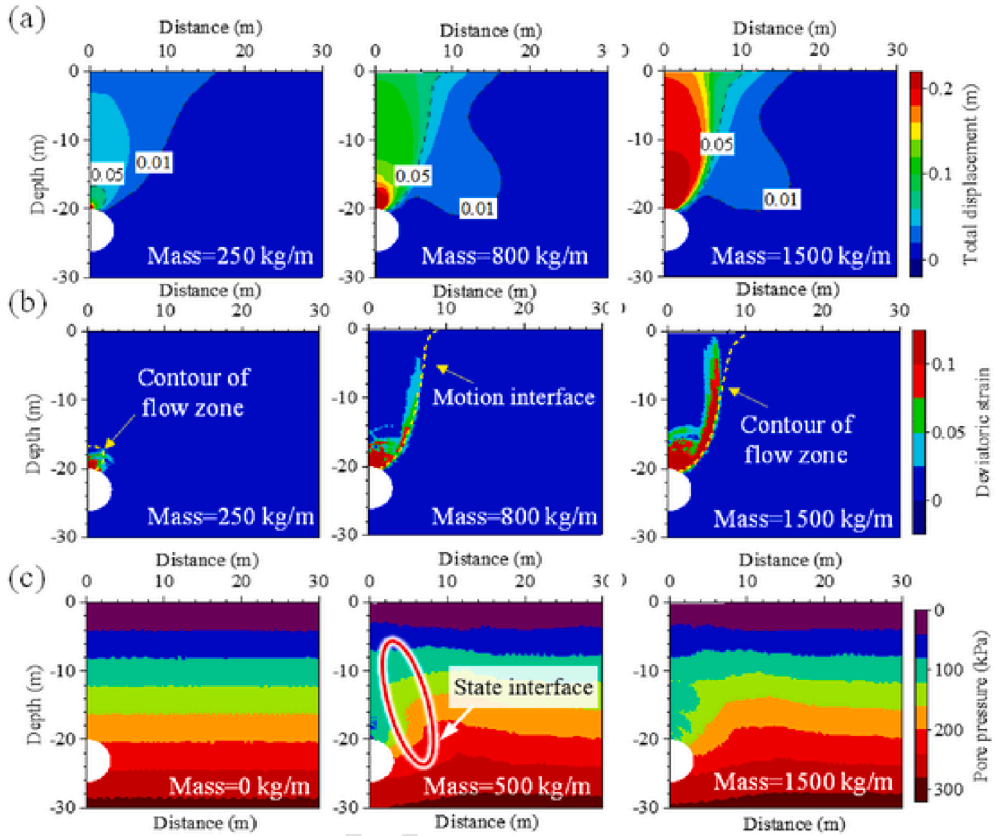

Fig. 24. The behavior of the geo-interfaces during gushing: (a) soil displacement, (b) deviatoric strain, and (c) pore water pressure (reproduced from Xie et al. (2022) with permission from Elsevier).

2020), thereby posing a significant threat to structures, underground pipelines, and other essential infrastructure. These fissures demonstrate complex geo-interface evolution, making them challenging to simulate with traditional numerical approaches. Therefore, employing advanced numerical methods in combination with mechanical theories is crucial for understanding the failure mechanisms of these geologic hazards.

Li et al. (2021a) improved the quasi-static MPM to simulate various behaviors of quasi-static cracks effectively in solid-phase materials on the basis of fracture mechanics. Building on this work, Li et al. (2023a) proposed a new approach to simulate earth fissures that considers factors such as consolidation and the size disparity between the fissure and the ground surface. Fig. 25 shows the MPM model along with its adaptive mesh refinement scheme. Additionally, the modified Duncan-Chang constitutive model was used to capture the motion interface of the soil because of its effectiveness in representing minor deformations in large model dimensions.

As shown in Fig. 26, the decreasing water levels caused differential subsidence. This led to a gradual concentration of tensile stress at the ground surface, initiating the formation of motion interfaces. As the water level continued to decrease, the area under tensile stress expanded. The first fissure formed in the region of maximum tensile stress, directly above the bedrock ridge, with the fissure line oriented nearly perpendicular to the soil surface. This fissure interface dynamically propagated, deepened and shifted in a zigzag pattern, driven by further reductions in water levels and changes in stress. This propagation continued until the stresses rebalanced. Occasionally, smaller fissure interfaces appeared on either side because of unresolved tensile stress in the surface soil. The fluctuations in groundwater levels critically influence the propagation and stabilization of these motion interfaces. The MPM effectively captures the complex interactions among changes in pore

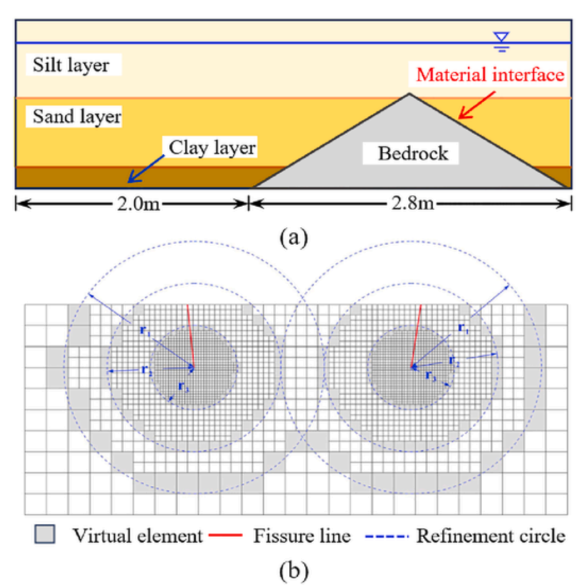

Fig. 25. (a) MPM modeling for a laboratory experiment of earth fissures and (b) three-level mesh refinement around fissure tips (adapted and reproduced from Li et al. (2023a) with permission from ASCE).

water pressure, soil deformation, and the development of geo-interfaces. This study provides a detailed quantification of the evolution of the geo-interface and supports the use of fracture mechanics to predict fracture development. This comprehensive approach significantly

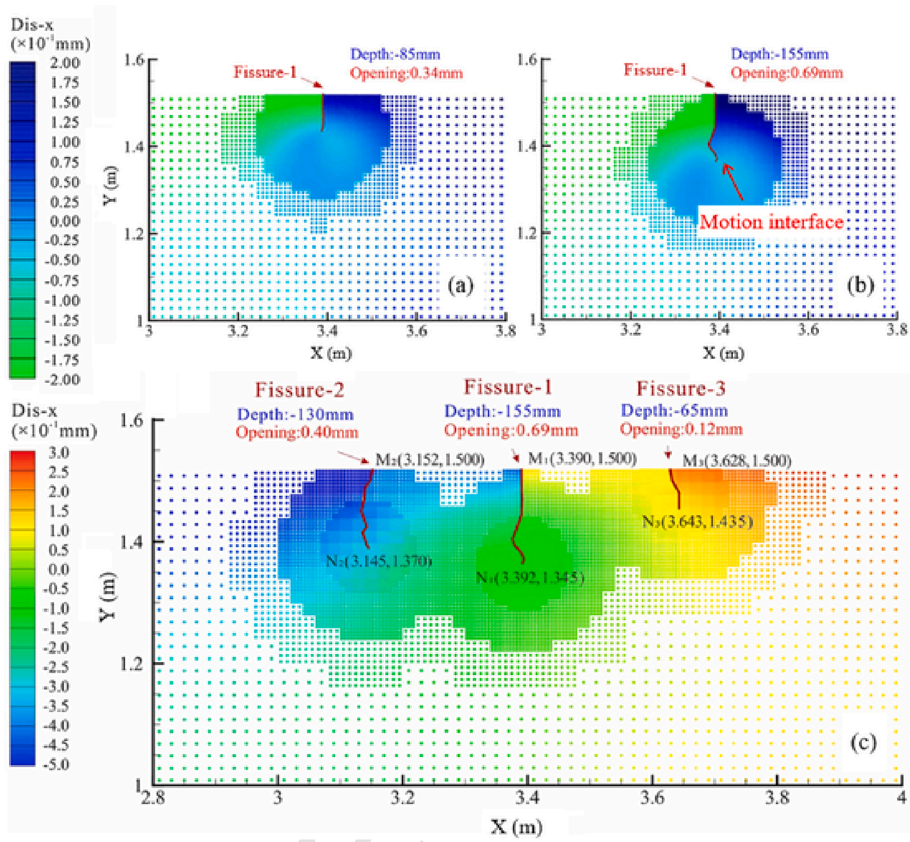

Fig. 26. (a, b) Accumulated displacement distribution during the first fissure growth and (c) final morphological characteristics of three earth fissures (reproduced from Li et al. (2023a) with permission from ASCE).

enhances the understanding of geo-interface behavior, which is crucial for investigating the failure mechanisms of human-induced geologic hazards.

8. Limitations and future research

8.1. Limitations

Despite significant advancements in the MPM for geo-interface modeling, several limitations and challenges still need to be addressed to further improve its simulation performance. Understanding these limitations is crucial for improving the predictive capabilities of the MPM and its practical applications in geo-interface modeling.

(1) In simulating material interfaces, many MPM applications employ relatively simplistic treatments for soil-structure interactions, which are primarily based on frictional contact algorithms. These methods may not accurately simulate complex geo-interfaces with varying material properties, limiting the accuracy of the simulations. Furthermore, in real geological structures, simulating material interfaces such as cracks and joints requires very small mesh elements, where significant scale differences pose modeling challenges.
(2) State interfaces often involve interactions among solid, liquid, and gas phases, necessitating coupled simulations to handle complex fluid-structure interactions. The MPM primarily uses Darcy's law to describe liquid motion within porous media, but this assumption is inadequate for modeling high-velocity flow conditions. Current MPM models also lack the ability to simulate thermal transfer at state interfaces, which is relevant to scenarios such as nuclear waste disposal or thermal effects in landslide movements. Furthermore, these models frequently overlook gas migration in unsaturated soil, which can significantly alter the mechanical and hydraulic properties of geo-interfaces. Neglecting these effects can lead to incomplete or inaccurate simulation results.
(3) To perform high-fidelity modeling of motion interfaces, the selection of appropriate constitutive models is crucial. At present, relatively simple models such as the MC and DP models are normally used in the MPM. Unfortunately, idealized constitutive models often fail to describe nonlinear stress-strain relationships and capture the complex evolution of motion interfaces, resulting in less reliable predictions. Factors such as strain rate, strain hardening/softening, and anisotropy significantly impact the evolution of motion interfaces, particularly during transitions between solid-like and fluid-like behaviors. In addition, simulating interactions at interfaces, such as frictional sliding, debonding, and rebonding, requires sophisticated contact algorithms that can handle large displacements and rotations.

8.2. Future research

To overcome the limitations of the MPM in modeling geo-interfaces previously discussed, future research should focus on enhancing the applicability of the MPM to complex geo-interface problems as follows:

(1) Combining the MPM with other numerical techniques, such as the FEM, DEM, SPH, CFD, PD, MD, and DDA, holds significant promise. These hybrid methods represent an area of ongoing research. By integrating the strengths of each technique, this

approach can facilitate multiscale and multiphysics simulations of geo-interfaces, significantly advancing our understanding of the evolution of various geo-interfaces.

(2) The incorporation of advanced constitutive models that account for anisotropy, nonlinearity, and time dependence in the MPM is particularly critical. These models can capture the evolution of motion interfaces during large deformations with greater accuracy. Furthermore, integrating the interface and structural elements of the FEM into the MPM is essential for overcoming the limitations of contact algorithms. This is necessary for modeling the material interfaces between soil and structures (e.g. piles, anchors, geogrids). These enhancements significantly increase the applicability of MPM in addressing complex geotechnical engineering challenges.

(3) Modeling air as a free-phase state is essential for detailed simulations of phase interactions and transitions, such as drying or wetting fronts in soil, landfill gas migration, and air expulsion from dam foundations during rapid drawdown. Furthermore, the rapid development of artificial intelligence (AI) techniques has led many researchers to combine AI with numerical simulation methods for studying geotechnical engineering problems (Kounlavong et al., 2023; Lu et al., 2023; Nguyen et al., 2023; Kim et al., 2024; Zhou et al., 2024). This technique can enhance the predictive capabilities of geo-interface models and assist in identifying patterns within large datasets, thus increasing the accuracy and reliability of MPM simulations.

Advancing these research areas will significantly improve geo-interface MPM modeling, leading to better predictions and management of geological hazards and contributing to safer engineering practices.

9. Conclusions

Geo-interfaces and their interaction mechanisms play pivotal roles in inducing various geological hazards. Simulating these interfaces is a key scientific issue in the field of geohazard mitigation and prevention. This review aims to provide a comprehensive overview of the basic concepts, classifications, and primary characteristics of geo-interfaces, along with the fundamental principles, various frameworks, limitations, and future research directions of MPM modeling. Additionally, this paper provides several applications of geo-interface analysis using the MPM. The main conclusions of this review are as follows:

(1) The MPM has demonstrated promising capabilities in simulating the behavior of geo-interfaces, primarily because of its significant advantages in modeling large deformations. By simulating different types of geo-interfaces (i.e. material, state, and motion interfaces), the MPM has proven effective in modeling soil-structure interactions and geohazards, such as landslides and earth fissures. This makes it a powerful tool for predicting geological disasters and enhancing risk assessment and management.

(2) Although the MPM has achieved significant progress in simulating the behavior of geo-interfaces, it still faces challenges related to simulation accuracy, computational efficiency, and multi-physics coupling. Current models are limited in their ability to handle complex boundary conditions, non-linear material deformations, and issues related to long time scales. To address these challenges, future research should focus on optimizing the MPM by introducing advanced constitutive models, developing more efficient numerical codes, and enhancing capabilities for multi-physics coupling.

(3) With the advancement of various numerical techniques, integrating the MPM with other simulation methods can significantly increase the accuracy and effectiveness of modeling geo-interfaces. Furthermore, the incorporation of AI techniques into MPM can optimize parameter selection and result analysis, thereby significantly improving the efficiency of predicting geo-interface behavior.

Uncited References

Abe et al., 2014; Beuth et al., 2007; Harlow, 1962; Zhang et al., 2009

CRediT authorship contribution statement

Tiancheng Xie: Writing – review & editing, Writing – original draft, Validation, Investigation. **Honghu Zhu:** Writing – review & editing, Writing – original draft, Validation, Methodology, Investigation, Funding acquisition, Conceptualization. **Youkou Dong:** Writing – review & editing, Investigation, Conceptualization. **Mingliang Zhou:** Writing – review & editing, Investigation, Funding acquisition, Conceptualization. **Bin Wang:** Writing – review & editing, Investigation, Conceptualization. **Wei Zhang:** Writing – review & editing, Investigation, Conceptualization. **Jidong Zhao:** Writing – review & editing, Investigation, Conceptualization.

Declaration of competing interest

The authors declare that they have no known competing financial interests or personal relationships that could have appeared to influence the work reported in this paper.

Acknowledgments

This work was financially supported by the National Science Fund for Distinguished Young Scholars of China (Grant No. 42225702) and the National Natural Science Foundation of China (Grant Nos. 42461160266 and 52379106). We thank Chunxin Zhang at Zhejiang University and Xinfei Jiang at Nanjing University for their kind support and suggestions in the revised version.

References

Abe K., Konagai K. Numerical simulation for runout process of debris flow using depth-averaged material point method. Soils Found. 2016;56(5):869–88.
Abe K., Soga K., Bandara S. Material point method for coupled hydromechanical problems. J. Geotech. Geoenviron. Eng. 2014;140(3):04013033.
Acosta J.G., Vardon P.J., Hicks M.A. Study of landslides and soil-structure interaction problems using the implicit material point method. Eng. Geol. 2021a;285:106043.
Acosta J.L.G., Vardon P.J., Hicks M.A. Development of an implicit contact technique for the material point method. Comput. Geotech. 2021b;130:103859.
Al-Kafaji K.I. Formulation of a Dynamic Material Point Method (MPM) for Geomechanical Problems. Stuttgart, Germany: Univ. of; 2013. PhD thesis.
Alsardi A., Yerro A. Coseismic site response and slope instability using periodic boundary conditions in the material point method. J. Rock Mech. Geotech. Eng. 2023;15(3): 641–58.
Alvarado M., Pinyol N.M., Alonso E.E. Landslide motion assessment including rate effects and thermal interactions: revisiting the Canelles landslide. Can. Geotech. J. 2019;56(9):1338–50.
Andersen S., Andersen L. Modelling of landslides with the material-point method. Comput. Geosci. 2010;14:137–47.
Anura3D. Anura3D MPM software v_2020; 2020. www.anura3d.com.
Bandara S., Ferrari A., Laloui L. Modelling landslides in unsaturated slopes subjected to rainfall infiltration using material point method. Int. J. Numer. Anal. Methods GeoMech. 2016;40(9):1358–80.
Bandara S., Soga K. Coupling of soil deformation and pore fluid flow using material point method. Comput. Geotech. 2015;63:199–214.
Bardenhagen S.G. An improved contact algorithm for the material point method and application to stress propagation in granular material. Comput. Model. Eng. Sci. 2001;2(4):509.
Bardenhagen S.G., Brackbill J.U., Sulsky D. The material-point method for granular materials. Comput. Methods Appl. Mech. Eng. 2000;187(3–4):529–41.
Bardenhagen S.G., Kober E.M. The generalized interpolation material point method. Comput. Model. Eng. Sci. 2004;5:477–96.
Baumgarten A.S., Kamrin K. Analysis and mitigation of spatial integration errors for the

material point method. Int. J. Numer. Methods Eng. 2023;1–49.
Beuth L. Formulation and Application of a Quasi-Static Material Point Method. Germany: Stuttgart University; 2012. PhD thesis.
Beuth L., Benz T., Vermeer P.A., Coetzee C.J., Bonnier P., van den Berg P. Formulation and validation of a quasi-static material point method. 10th International Symposium in Numerical Methods in GeoMechanics. Rhodes, Greece; 2007. p. 189–95.
Beuth L., Więckowski Z., Vermeer P.A. Solution of quasi-static large-strain problems by the material point method. Int. J. Numer. Anal. Methods GeoMech. 2011;35(13): 1451–65.
Bhandari T., Hamad F., Moormann C., Sharma K.G., Westrich B. Numerical modelling of seismic slope failure using MPM. Comput. Geotech. 2016;75:126–34.
Bishop A.W. The use of the slip circle in the stability analysis of earth slopes. Geotechnique 1955;5(1):7–17.
Bisht V., Salgado R., Prezzi M. Simulating penetration problems in incompressible materials using the material point method. Comput. Geotech. 2021;133:103593.
Bojanowski C. Numerical modeling of large deformations in soil structure interaction problems using FE, EFG, SPH, and MM-ALE formulations. Arch. Appl. Mech. 2014;84: 743–55.
Budhu M. Mechanics of earth fissures using the Mohr-Coulomb failure criterion. Environ. Eng. Geosci. 2008;14(4):281–95.
Ceccato F., Beuth L., Simonini P. Analysis of piezocone penetration under different drainage conditions with the two-phase material point method. J. Geotech. Geoenviron. Eng. 2016;142:04016066.
Ceccato F., Bisson A., Cola S. Large displacement numerical study of 3D plate anchors. Eur. J. Environ. Civ. Eng. 2020;24:520–38.
Ceccato F., Redaelli I., di Prisco C., Simonini P. Impact forces of granular flows on rigid structures: comparison between discontinuous (DEM) and continuous (MPM) numerical approaches. Comput. Geotech. 2018a;103:201–17.
Ceccato F., Simonini P. Numerical study of partially drained penetration and pore pressure dissipation in piezocone test. Acta Geotech 2017;12:195–209.
Ceccato F., Yerro A., Di Carluccio G. Simulating landslides with the material point method: best practices, potentialities, and challenges. Eng. Geol. 2024;107614.
Ceccato F., Yerro A., Martinelli M. Modelling soil-water interaction with the material point method. Evaluation of Single-point and Double-point Formulations. CRC Press; 2018b. p. 351.
Chaloulos Y.K., Bouckovalas G.D., Karamitros D.K. Trench effects on lateral py relations for pipelines embedded in stiff soils and rocks. Comput. Geotech. 2017;83:52–63.
Chaloulos Y.K., Bouckovalas G.D., Zervos S.D., Zampas A.L. Lateral soil–pipeline interaction in sand backfill: effect of trench dimensions. Comput. Geotech. 2015;69: 442–51.
Charlton T., Coombs W., Augarde C. IGIMP: an implicit generalised interpolation material point method for large deformations. Comput. Struct. 2017;190:108–25.
Chen H., Zhao S., Zhao J., Zhou X. DEM-enriched contact approach for material point method. Comput. Methods Appl. Mech. Eng. 2023;404:115814.
Chen J.S., Hillman M., Chi S.W. Meshfree methods: progress made after 20 years. J. Eng. Mech. 2017;143:04017001.
Chen X., Li D., Tang X., Liu Y. A three-dimensional large-deformation random finite-element study of landslide runout considering spatially varying soil. Landslides 2021; 18(9):3149–62.
Chen Y., Zhao W., Han J., Jia P. A CEL study of bearing capacity and failure mechanism of strip footing resting on c-φ soils. Comput. Geotech. 2019;111:126–36.
Cheng W.C., Li G., Liu N., Xu J., Horpibulsuk S. Recent massive incidents for subway construction in soft alluvial deposits of Taiwan: a review. Tunn. Undergr. Space Technol. 2020;96:103178.
Cheon Y.J., Kim H.G. An efficient contact algorithm for the interaction of material particles with finite elements. Comput. Methods Appl. Mech. Eng. 2018;335:631–59.
Chu L.M., Yin J.H. Comparison of interface shear strength of soil nails measured by both direct shear box tests and pullout tests. J. Geotech. Geoenviron. Eng. 2005;131(9): 1097–107.
Coetzee C.J., Vermeer P.A., Basson A.H. The modelling of anchors using the material point method. Int. J. Numer. Anal. Methods GeoMech. 2005;29:879–95.
Conte E., Pugliese L., Troncone A. Post-failure stage simulation of a landslide using the material point method. Eng. Geol. 2019;253:149–59.
Conte E., Pugliese L., Troncone A. Post-failure analysis of the Maierato landslide using the material point method. Eng. Geol. 2020;277:105788.
Cuomo S., Di Perna A., Martinelli M. MPM modelling of buildings impacted by landslides. Workshop on World Landslide Forum. Springer; 2021a. p. 245–66.
Cuomo S., Di Perna A., Martinelli M. Material point method (MPM) hydro-mechanical modelling of flows impacting rigid walls. Can. Geotech. J. 2021b;58(11):1730–43.
Cuomo S., Di Perna A., Martinelli M. Modelling the spatio-temporal evolution of a rainfall-induced retrogressive landslide in an unsaturated slope. Eng. Geol. 2021c; 294:106371.
Cuomo S., Di Perna A., Martinelli M. Analytical and numerical models of debris flow impact. Eng. Geol. 2022;308:106818.
Cuomo S., Di Perna A., Moscariello A., Martinelli M. Possible remediation of impact-loading debris avalanches via fine long rooted grass: an experimental and material point method (MPM) analysis. Landslides 2023;21(4):679–96.
Cuomo S., Di Perna A., Savino S., Frigo B., Martinelli M. Reinforced embankments impacted by landslides: analytical and numerical modelling. Geosynthetics: Leading the Way to a Resilient Planet 2024;915–21.
Day R.A., Potts D.M. Zero thickness interface elements—numerical stability and application. Int. J. Numer. Anal. Methods GeoMech. 1994;18:689–708.
de Vaucorbeil A., Nguyen V.P., Sinaie S., Wu J.Y. Material point method after 25 years: theory, implementation, and applications. Adv. Appl. Mech. 2020;53:185–398.
DeJong J.T., White D.J., Randolph M.F. Microscale observation and modeling of soil-structure interface behavior using particle image velocimetry. Soils Found. 2006;46: 15–28.
Deng L.C., Zhang W., Deng L., Shi Y.H., Zi J.J., He X., Zhu H.H. Forecasting and early warning of shield tunnelling-induced ground collapse in rock-soil interface mixed ground using multivariate data fusion and Catastrophe Theory. Eng. Geol. 2024;335: 107548.
Desai C.S., Zaman M.M., Lightner J.G., Siriwardane H.J. Thin-layer element for interfaces and joints. Int. J. Numer. Anal. Methods GeoMech. 1984;8:19–43.
Dhadse G.D., Ramtekkar G., Bhatt G. A succinct review on soil structure interface thickness. Arch. Comput. Methods Eng. 2023;1–8.
Dhadse G.D., Ramtekkar G.D., Bhatt G. Finite element modeling of soil structure interaction system with interface: a review. Arch. Comput. Methods Eng. 2021;28: 3415–32.
Dong Y. Reseeding of particles in the material point method for soil–structure interactions. Comput. Geotech. 2020;127:103716.
Dong Y., Wang D., Cui L. Assessment of depth-averaged method in analysing runout of submarine landslide. Landslides 2020a;17:543–55.
Dong Y., Wang D., Randolph M.F. A GPU parallel computing strategy for the material point method. Comput. Geotech. 2015;66:31–8.
Dong Y., Wang D., Randolph M.F. Investigation of impact forces on pipeline by submarine landslide using material point method. Ocean. Eng. 2017a;146:21–8.
Dong Y., Wang D., Randolph M.F. Runout of submarine landslide simulated with material point method. J. Hydrodyn. 2017b;29(3):438–44.
Dong Y., Wang D., Randolph M.F. Quantification of impact forces on fixed mudmats from submarine landslides using the material point method. Appl. Ocean Res. 2020b; 102:102227.
Du W., Sheng Q., Fu X., Chen J., Wei P., Zhou Y. Post-failure analysis of landslide blocking river using the two-phase double-point material point method: a case of western Hubei, China. Bull. Eng. Geol. Environ. 2023;82(3):98.
Du W., Sheng Q., Fu X., Chen J., Zhou Y. Extensions of the two-phase double-point material point method to simulate the landslide-induced surge process. Eng. Anal. Bound. Elem. 2021;133:362–75.
Duncan J.M. State of the art: limit equilibrium and finite element analysis of slopes. J. Geotech. Eng. 1996;122(7):577–96.
Ettema R., Baker M.E., Teal M., Trojanowski J. Ice-Run destruction of spencer dam on Nebraska's niobrara river. CGU HS Committee on River Ice Processes and the Environment, 21st Workshop on the Hydraulics of Ice-Covered Rivers, Saskatoon, Saskatchewan, Canada; 2024.
Fang K., Dong A., Tang H., An P., Wang Q., Jia S., Zhang B. Development of an easy-assembly and low-cost multismartphone photogrammetric monitoring system for rock slope hazards. Int. J. Rock Mech. Min. Sci. 2024;174:105655.
Feng K., Huang D., Wang G. Two-layer material point method for modeling soil–water interaction in unsaturated soils and rainfall-induced slope failure. Acta Geotech 2021; 16(8):2529–51.
Feng Z.K., Xu W.J. GPU material point method (MPM) and its application on slope stability analysis. Bull. Eng. Geol. Environ. 2021;80(7):5437–49.
Fern E.J., de Lange D.A., Zwanenburg C., Teunissen J.A.M., Rohe A., Soga K. Experimental and numerical investigations of dyke failures involving soft materials. Eng. Geol. 2017;219:130–9.
Fern J., Rohe A., Soga K., Alonso E. The Material Point Method for Geotechnical Engineering: A Practical Guide. CRC Press; 2019.
Fernández F., do Amaral Vargas E., Quadros Velloso R. A 3D discretization procedure for the material point method (MPM). Comput. Particle Mech. 2020;7:725–33.
Fernández F., Vargas Jr E., Muller A.L., Sousa R.L., Sousa L.R. Material point method modeling in 3D of the failure and run-out processes of the Daguangbao landslide. Acta Geotech 2023;1–20.
Frost J.D., DeJong J.T., Recalde M. Shear failure behavior of granular–continuum interfaces. Eng. Fract. Mech. 2002;69(17):2029–48.
Frost J.D., Han J. Behavior of interfaces between fiber reinforced polymers and sands. J. Geotech. Geoenviron. Eng. 1999;125(8):633–40.
Frost J.D., Hebeler G.L., Evans T.M., DeJong J.T. Interface behavior of granular soils. Proc. Earth and Space Conference; 2004. p. 65–72. Houston, TX.
Fu S., Yang Z.X., Guo N., Jardine R.J. Material point method simulations of displacement pile and CPT penetration in sand considering the effects of grain breakage. Comput. Geotech. 2024;166:105945.
Galavi V., Martinelli M. MPM simulation of the installation of an impact-driven pile in dry sand and subsequent axial bearing capacity. J. Geotech. Geoenviron. Eng. 2024; 150(4):04024019.
Gao L., Liao D., Mo P.Q. Modeling footing resting on anisotropic sand using material point method. J. Rock Mech. Geotech. Eng. 2023;15(12):3271–90.
Gazetas G., Tassoulas J. Horizontal stiffness of arbitrarily shaped embedded foundations. J. Geotech. Eng. 1987;113(5):440–57.
Girardi V., Ceccato F., Rohe A., Simonini P., Gabrieli F. Failure of levees induced by toe uplift: investigation of post-failure behavior using material point method. J. Rock Mech. Geotech. Eng. 2023;15(4):970–83.
Girardi V., Yerro A., Ceccato F., Simonini P. Modelling deformations in water retention structures with unsaturated material point method. Proc. Inst. Civ. Eng. Geotech. Eng. 2021;174(5):577–92.
Given J., Liang Y., Zeng Z., Zhang X., Soga K. The virtual stress boundary method to impose nonconforming Neumann boundary conditions in the material point method. Comp. Part. Mech 2024;1–25.
Goodman R.E., Shi G. Block Theory and its Application to Rock Engineering. New Jersey, USA: Prentice-Hall Inc.; 1985.
Goodman R.E., Taylor R.L., Brekke T.L. A model for the mechanics of jointed rock. J. Soil Mech. Found Div. 1968;94(3):637–59.
Guilkey J.E., Weiss J.A. Implicit time integration for the material point method: quantitative and algorithmic comparisons with the finite element method. Int. J.

Numer. Methods Eng. 2003;57(9):1323–38.
Harlow F.H. The Particle-In-Cell Method for Numerical Solution of Problems in Fluid Dynamics. Los Alamos, NM (United States): Los Alamos National Lab. (LANL); 1962. LADC-5288.
Hashimoto R., Bodhinanda C., Soga K. A coupled implicit MPM-DDA for soil-structure interaction problems. Proc. WCCM-APCOM 2714; 2022.
He M., e Sousa L.R., Müller A., Vargas Jr E., Sousa R.L., Oliveira C.S., Gong W. Numerical and safety considerations about the Daguangbao landslide induced by the 2008 Wenchuan earthquake. J. Rock Mech. Geotech. Eng. 2019;11(5):1019–35.
Higo Y., Oka F., Kimoto S., Morinaka Y., Goto Y., Chen Z. A coupled MPM-FDM analysis method for multi-phase elasto-plastic soils. Soils Found. 2010;50(4):515–32.
Hosseini M.R., Martek I., Zavadskas E.K., Aibinu A.A., Arashpour M., Chileshe N. Critical evaluation of off-site construction research: a Scientometric analysis. Autom. ConStruct. 2018;87:235–47.
Hu L., Pu J. Testing and modeling of soil-structure interface. J. Geotech. Geoenviron. Eng. 2004;130(8):851–60.
Hu W., Huang R., McSaveney M., Yao L., Xu Q., Feng M., Zhang X. Superheated steam, hot CO2 and dynamic recrystallization from frictional heat jointly lubricated a giant landslide: field and experimental evidence. Earth Planet Sci. Lett. 2019;510:85–93.
Hu X., Bürgmann R., Schulz W.H., Fielding E.J. Four-dimensional surface motions of the Slumgullion landslide and quantification of hydrometeorological forcing. Nat. Commun. 2020;11:2792.
Huang B., Liu J., Fan J., Ling D. Experimental study on uplift mechanisms of pipes buried in sloping medium dense sand. J. Pipeline Syst. Eng. Pract. 2021;12(3): 04021027.
Huang B., Liu J., Ling D., Zhou Y. Application of particle image velocimetry (PIV) in the study of uplift mechanisms of pipe buried in medium dense sand. J. Civ. Struct. Health Monit. 2015;5(5):599–614.
Huang L., Ma J., Lei M., Liu L., Lin Y., Zhang Z. Soil-water inrush induced shield tunnel lining damage and its stabilization: a case study. Tunn. Undergr. Space Technol. 2020;97:103290.
Huo Y.X., Gomaa S.M., Zayed T., Meguid M. Review of analytical methods for stress and deformation analysis of buried water pipes considering pipe-soil interaction. Undergr. Space 2023;13:205–27.
Jakob M., Stein D., Ulmi M. Vulnerability of buildings to debris flow impact. Nat. Hazards 2012;60(2):241–61.
Jassim I., Stolle D., Vermeer P. Two-phase dynamic analysis by material point method. Int. J. Numer. Anal. Methods GeoMech. 2013;37(15):2502–22.
Jiang Y., Li M., Jiang C., Alonso-Marroquin F. A hybrid material-point spheropolygon-element method for solid and granular material interaction. Int. J. Numer. Methods Eng. 2020;121(14):3021–47.
Jiang Y., Zhao Y., Choi C.E., Choo J. Hybrid continuum-discrete simulation of granular impact dynamics. Acta Geotech 2022;17:5597–612.
Kalantari A.R., Johari A., Zandpour M., Kalantari M. Effect of spatial variability of soil properties and geostatistical conditional simulation on reliability characteristics and critical slip surfaces of soil slopes. Transp. Geotech. 2023;39:100933.
Kim D., Kim T., Kim Y., Byun Y.H., Yun T.S. A ChatGPT-MATLAB framework for numerical modeling in geotechnical engineering applications. Comput. Geotech. 2024;169:106237.
King L., Bouazza A., Maksimenko A., Gates W.P., Dubsky S. Measurement of three-dimensional displacement field in piled embankments using synchrotron X-ray tomography. Can. Geotech. J. 2019;56(6):885–92.
Kiriyama T., Higo Y. Arbitrary particle domain interpolation method and application to problems of geomaterial deformation. Soils Found. 2020;60(6):1422–39.
Kirschbaum D.B., Adler R., Hong Y., Hill S., Lerner-Lam A. A global landslide catalog for hazard applications: method, results, and limitations. Nat. Hazards 2010;52(3): 561–75.
Kounlavong K., Chavda J.T., Jamsawang P., Keawsawasvong S. Stability analysis of buried pipelines under combined uplift and lateral forces using FELA and ANN. Appl. Ocean Res. 2023;135:103568.
Le T.C., Liu C., Tang C.S., Zhang X.Y., Shi B. Numerical simulation of desiccation cracking in clayey soil using a multifield coupling discrete-element model. J. Rock Mech. Geotech. Eng. 2022;148(2):04021183.
Lee M., Martinelli M., Shieh C.L. Modelling rainfall-induced landslides with the material point method: the Fei Tsui Road case. Proceedings of the XVII ECSMGE; 2019a.
Lee M., Martinelli M., Shieh C.L. Numerical Analysis of the Shiaolin Landslide using material point method. 7th International Symposium on Geotechnical Safety and Risk; 2019b. p. 11–3.
Lee M., Martinelli M., Shieh C.L. An investigation of rainfall-induced landslides from the pre-failure stage to the post-failure stage using the material point method. Front. Earth Sci. 2021;9:764393.
Lenardic A., Moresi L., Muhlhaus H. The role of mobile belts for the longevity of deep cratonic lithosphere: the crumpled zone model. Geophys. Res. Lett. 2000;27(8): 1235–8.
Li J., Wang B., Pan P., Chen H., Wang D., Chen P. Failure analysis of soil-rock mixture slopes using coupled MPM-DEM method. Comput. Geotech. 2024;169:106226.
Li S., Zhang Y., Wu J., Yu J., Gong X. Modeling of crack propagation with the quasi-static material point method. Eng. Fract. Mech. 2021a;245:107602.
Li S., Zhang Y., Wu J., Yu J., Gong X. Numerical modeling of pumping-induced earth fissures using coupled quasi-static material point method. J. Geotech. Geoenviron. Eng. 2023a;149(9):04023065.
Li W.L., Guo N., Yang Z.X., Helfer T. Large-deformation geomechanical problems studied by a shear-transformation-zone model using the material point method. Comput. Geotech. 2021b;135:104153.
Li X., Fang Y., Li M., Jiang C. BFEMP: interpenetration-free MPM–FEM coupling with barrier contact. Comput. Methods Appl. Mech. Eng. 2022a;390:114350.
Li X., Wu Y., He S., Su L. Application of the material point method to simulate the post-failure runout processes of the Wangjiayan landslide. Eng. Geol. 2016;212:1–9.
Li X., Yan Q., Zhao S., Luo Y., Wu Y., Wang D. Investigation of influence of baffles on landslide debris mobility by 3D material point method. Landslides 2020;17:1129–43.
Li X., Yao J., Sun Y., Wu Y. Material point method analysis of fluid–structure interaction in geohazards. Nat. Hazards 2022;114:3425–43.
Li Z., Huang H., Zhou M., Zhang D. Failure responses of rock tunnel faces during excavation through the fault-fracture zone. Undergr. Space 2023b;10:166–81.
Lian Y., Zhang X., Zhou X., Ma Z. A FEMP method and its application in modeling dynamic response of reinforced concrete subjected to impact loading. Comput. Methods Appl. Mech. Eng. 2011;200(17–20):1659–70.
Liang D., Zhao X., Soga K. Simulation of overtopping and seepage induced dike failure using two-point MPM. Soils Found. 2020;60:978–88.
Liang W., Wu H., Zhao S., Zhou W., Zhao J. Scalable three-dimensional hybrid continuum-discrete multiscale modeling of granular media. Int. J. Numer. Methods Eng. 2022;123:2872–93.
Liang W., Zhao J. Multiscale modeling of large deformation in geomechanics. Int. J. Numer. Anal. Methods GeoMech. 2019;43(5):1080–114.
Liang W., Zhao J., Wu H., Soga K. Multiscale, multiphysics modeling of saturated granular materials in large deformation. Comput. Methods Appl. Mech. Eng. 2023a; 405:115871.
Liang Y., Given J., Soga K. The imposition of nonconforming Neumann boundary condition in the material point method without boundary representation. Comput. Methods Appl. Mech. Eng. 2023b;404:115785.
Liao Z., Ren M., Tang C., Zhu J. A three-dimensional damage-based contact element model for simulating the interfacial behaviors of rocks and its validation and applications. Geomech Geophys Geo-Energy Geo-Resour. 2020;6(3):1–21.
Liu C., Sun Q., Jin F., Zhou G.G. A fully coupled hydro-mechanical material point method for saturated dense granular materials. Powder Technol. 2017;314:110–20.
Liu C., Sun Q., Zhou G.G.D. Coupling of material point method and discrete element method for granular flows impacting simulations. Int. J. Numer. Methods Eng. 2018; 115:172–88.
Liu K., Wang Y., Huang M., Yuan W.H. Postfailure analysis of slopes by random generalized interpolation material point method. Int. J. GeoMech. 2021;21: 04021015.
Liu L.L., Zhang P., Zhang S.H., Li J.Z., Huang L., Cheng Y.M., Wang B. Efficient evaluation of run-out distance of slope failure under excavation. Eng. Geol. 2022;306: 106751.
Liu X., Wang Y. Probabilistic simulation of entire process of rainfall-induced landslides using random finite element and material point methods with hydro-mechanical coupling. Comput. Geotech. 2021;132:103989.
Liu X., Wang Y., Li D.Q. Investigation of slope failure mode evolution during large deformation in spatially variable soils by random limit equilibrium and material point methods. Comput. Geotech. 2019;111:301–12.
Liu X., Wang Y., Li D.Q. Numerical simulation of the 1995 rainfall-induced Fei Tsui Road landslide in Hong Kong: new insights from hydro-mechanically coupled material point method. Landslides 2020;17:2755–75.
Llano-Serna M.A., Farias M.M., Pedroso D.M. An assessment of the material point method for modelling large scale run-out processes in landslides. Landslides 2016;13: 1057–66.
Locat J., Lee H.J. Submarine landslides: advances and challenges. Can. Geotech. J. 2002; 39(1):193–212.
Lu M., Ceccato F., Zhou M., Yerro A., Zhang J. Evaluating the exceedance probability of the runout distance of rainfall-induced landslides using a two-stage FEM-MPM approach. Acta Geotech 2023;19:3691–706.
Luco J.E. A simple model for structural control including soil–structure interaction effects. Earthq. Eng. Struct. Dynam. 1998;27(3):225–42.
Luo G., Yan C., Li X., Jiang J., Ma J. Exploration of water resource and multiple model for water resource development in karst areas with the preferred plane theory. Acta Geol. Sin.-English Edit. 2003;77(1):129–35.
Lysmer J., Kuhlemeyer R.L. Finite dynamic model for infinite media. J. Eng. Mech. Div. 1969;95(4):859–77.
Ma J., Wang D., Randolph M.F. A new contact algorithm in the material point method for geotechnical simulations. Int. J. Numer. Anal. Methods GeoMech. 2014;38: 1197–210.
Martinelli M. Soil-water Interaction with Material Point Method. Double-point Formulation. 2016.
Martinelli M., Galavi V. Investigation of the material point method in the simulation of cone penetration tests in dry sand. Comput. Geotech. 2021;130:103923.
Martinelli M., Galavi V. An explicit coupled MPM formulation to simulate penetration problems in soils using quadrilateral elements. Comput. Geotech. 2022;145:104697.
Martinelli M., Lee M., Shieh C.L., Cuomo S. Rainfall boundary condition in a multiphase material point method. Workshop on World Landslide Forum. Springer; 2020. p. 303–9.
Martinelli M., Rohe A., Soga K. Modeling dike failure using the material point method. Procedia Eng. 2017a;175:341–8.
Martinelli M., Tehrani P.H., Galavi V. Analysis of crater development around damaged pipelines using the material point method. Procedia Eng. 2017b;175:204–11.
Mast C.M., Arduino P., Miller G.R., Mackenzie-Helnwein P. Avalanche and landslide simulation using the material point method: flow dynamics and force interaction with structures. Comput. Geosci. 2014;18:817–30.
Monzer A., Faramarzi A., Yerro A., Chapman D. MPM Investigation of the fluidization initiation and postfluidization mechanism around a pressurized leaking Pipe. J. Geotech. Geoenviron. Eng. 2023;149:04023096.
Nakamura K., Matsumura S., Mizutani T. Particle-to-surface frictional contact algorithm for material point method using weighted least squares. Comput. Geotech. 2021;134:

104069.
Nayroles B., Touzot G., Villon P. Generalizing the finite element method: diffuse approximation and diffuse elements. Comput. Mech. 1992;10(5):307–18.
Nguyen D.K., Nguyen T.P., Ngamkhanong C., Keawsawasvong S., Nguyen T.K. Prediction of uplift resistance of circular anchors in anisotropic clays using MLR, ANN, and MARS. Appl. Ocean Res. 2023;136:103584.
Nguyen T.S., Yang K.H., Wu Y.K., Teng F., Chao W.A., Lee W.L. Post-failure process and kinematic behavior of two landslides: case study and material point analyses. Comput. Geotech. 2022;148:104797.
Onyelowe K.C., Fazel Mojtahedi F., Golaghaei Darzi A., Kontoni D.P.N. Solving large deformation problems in geotechnical and geo-environmental engineering with the smoothed particle hydrodynamics: a state-of-the-art review of constitutive solutions. Environ. Earth Sci. 2023;82(17):394.
O'Rourke T.D. Geohazards and large, geographically distributed systems. Geotechnique 2010;60(7):505–43.
Pande G.N., Sharma K.G. On joint/interface elements and associated problems of numerical ill-conditioning. Int. J. Numer. Anal. Methods GeoMech. 1979;3(3): 293–300.
Paniagua P., Andó E., Silva M., Emdal A., Nordal S., Viggiani G. Soil deformation around a penetrating cone in silt. Géotech. Lett. 2013;3(4):185–91.
Pastor M., Tayyebi S.M., Stickle M.M., Yagüe N., Manzanal D. A depth integrated, coupled, two-phase model for debris flow propagation. Acta Geotech 2021;2:1–25.
Pastor M., Yague A., Stickle M.M., Manzanal D., Mira P. A two-phase SPH model for debris flow propagation. Int. J. Numer. Anal. Methods GeoMech. 2018;42(3):418–48.
Peng J., Sun X., Lu Q., Meng L., He H., Qiao J., Wang F. Characteristics and mechanisms for origin of earth fissures in Fenwei basin, China. Eng. Geol. 2020;266: 105445.
Perna A., Cuomo S., Martinelli M. Empirical formulation for debris flow impact and energy release. Geoenviron. Disasters 2022a;9(1):8.
Perna A., Cuomo S., Martinelli M. Impact forces and energy of flow-like landslides against protection barriers: a new MPM-validated empirical formulation. Geoenviron. Disasters 2022b.
Phuong N.T.V., Van Tol A.F., Elkadi A.S.K., Rohe A. Numerical investigation of pile installation effects in sand using material point method. Comput. Geotech. 2016;73: 58–71.
Qin J., Mei G., Xu N. Meshfree methods in geohazards prevention: a survey. Arch. Comput. Methods Eng. 2022;29(5):3151–82.
Qiu G., Henke S., Grabe J. Application of a Coupled Eulerian–Lagrangian approach on geomechanical problems involving large deformations. Comput. Geotech. 2011;38 (1):30–9.
Raymond S.J., Jones B., Williams J.R. A strategy to couple the material point method (MPM) and smoothed particle hydrodynamics (SPH) computational techniques. Comput. Particle Mech. 2016;5:49–58.
Reissner E. Stationare, axialsymmetrische, durch eine schuttelnde masses erregte schwingungen elastischen halbraumes. Arch. Appl. Mech. 1936;7(6):381–96.
Roy K., Hawlader B., Kenny S., Moore I. Upward pipe–soil interaction for shallowly buried pipelines in dense sand. J. Geotech. Geoenviron. Eng. 2018;144(11): 04018078.
Saberi M., Annan C.D., Konrad J.M. On the mechanics and modeling of interfaces between granular soils and structural materials. Arch. Civ. Mech. Eng. 2018;18: 1562–79.
Sadeghirad A., Brannon R.M., Burghardt J. Converted particle domain interpolation technique to extend applicability of the material point method for problems involving massive deformations. Int. J. Numer. Methods Eng. 2011;86:1435–56.
Sadeghirad A., Brannon R.M., Guilkey J. Second-order convected particle domain interpolation (CPDI2) with enrichment for weak discontinuities at material interfaces. Int. J. Numer. Methods Eng. 2013;95:928–52.
Saito H., Korup O., Uchida T., Hayashi S., Oguchi T. Rainfall conditions, typhoon frequency, and contemporary landslide erosion in Japan. Geology 2014;42(11): 999–1002.
Scaringi G., Fan X., Xu Q., Liu C., Ouyang C., Domènech G., Yang F., Dai L. Some considerations on the use of numerical methods to simulate past landslides and possible new failures: the case of the recent Xinmo landslide (Sichuan, China). Landslides 2018a;15:1359–75.
Scaringi G., Hu W., Xu Q., Huang R. Shear-rate-dependent behavior of clayey bimaterial interfaces at landslide stress levels. Geophys. Res. Lett. 2018b;45:766–77.
Scaringi G., Loche M. A thermo-hydro-mechanical approach to soil slope stability under climate change. Geomorphology 2022;401:108108.
Shen L., Chen Z. A silent boundary scheme with the material point method for dynamic analyses. Comput. Model. Eng. Sci. 2005;7(3):305–20.
Shi B., Zhang Y., Zhang W. Analysis of the entire failure process of the rotational slide using the material point method. Int. J. GeoMech. 2018;18(8):04018092.
Shi B., Zhang Y., Zhang W. Run-out of the 2015 Shenzhen landslide using the material point method with the softening model. Bull. Eng. Geol. Environ. 2019;78:1225–36.
Shi J.J., Zhang W., Wang B., Li C.Y., Pan B. Simulation of a submarine landslide using the coupled material point method. Math. Probl Eng. 2020;2020:1–14.
Sim W.W., Towhata I., Yamada S. One-g shaking-table experiments on buried pipelines crossing a strike-slip fault. Geotechnique 2012;62(12):1067–79.
Soga K., Alonso E., Yerro A., Kumar K., Bandara S. Trends in large-deformation analysis of landslide mass movements with particular emphasis on the material point method. Geotechnique 2016;66(3):248–73.
Sołowski W.T., Berzins M., Coombs W.M., Guilkey J.E., Möller M., Tran Q.A., Adibaskoro T., Seyedan S., Tielen R., Soga K. Material point method: overview and challenges ahead. Adv. Appl. Mech. 2021;54:113–204.
Steffen M., Kirby R.M., Berzins M. Analysis and reduction of quadrature errors in the material point method (MPM). Int. J. Numer. Methods Eng. 2008;76(6):922–48.
Steffffen M., Wallstedt P., Guilkey J., Kirby R., Berzins M. Examination and analysis of implementation choices within the material point method (MPM). Comput. Model. Eng. Sci. 2008;31:107–27.
Sulsky D., Chen Z., Schreyer H.L. A particle method for history-dependent materials. Comput. Methods Appl. Mech. Eng. 1994;118(1–2):179–96.
Talmon M., Martinelli M., Luger D. Numerical simulation of cutting tests on layered sand and clay. Proc. 22nd World Dredging Congress; 2019. Shanghai, China.
Tan D.Y., Yin J.H., Feng W.Q., Zhu Z.H., Qin J.Q., Chen W.B. New simple method for calculating impact force on flexible barrier considering partial muddy debris flow passing through. J. Geotech. Geoenviron. Eng. 2019;145(9):04019051.
Tan Y., Lu Y. Forensic diagnosis of a leaking accident during excavation. J. Perform. Constr. Facil. 2017;31:04017061.
Tang C.S., Zhu C., Cheng Q., Zeng H., Xu J.J., Tian B.G., Shi B. Desiccation cracking of soils: a review of investigation approaches, underlying mechanisms, and influencing factors. Earth Sci. Rev. 2021;216:103586.
Tariq S., Hu Z., Zayed T. Micro-electromechanical systems-based technologies for leak detection and localization in water supply networks: a bibliometric and systematic review. J. Clean. Prod. 2021;289:125751.
Tran Q.A., Grimstad G., Ghoreishian Amiri S.A. MPMICE: a hybrid MPM-CFD model for simulating coupled problems in porous media. Application to earthquake-induced submarine landslides. Int. J. Numer. Methods Eng. 2024;125(5):e7383.
Tran Q.A., Sołowski W. Temporal and null-space filter for the material point method. Int. J. Numer. Methods Eng. 2019;120(3):328–60.
Tu S., Li W., Zhang C., Wang L., Wang S., Zhao Y., Wu J. Face stability analysis of tunnels in saturated soil considering soil-fluid coupling effect via material point method. Comput. Geotech. 2023;161:105592.
Uesugi M., Kishida H., Tsubakihara Y. Behavior of sand particles in sand-steel friction. Soils Found. 1988;28(1):107–18.
Vermeer P.A., Yuan Y., Beuth L., Bonnier P. Application of interface elements with the material point method. 18th Int. Conf. Soil Mech. Geotech. Eng., Paris, France; 2009.
Vicari H., Tran Q.A., Nordal S., Thakur V. MPM modelling of debris flow entrainment and interaction with an upstream flexible barrier. Landslides 2022;19(9):2101–15.
Wang B., Vardon P.J., Hicks M.A. Investigation of retrogressive and progressive slope failure mechanisms using the material point method. Comput. Geotech. 2016a;78: 88–98.
Wang B., Vardon P.J., Hicks M.A. Preliminary analysis of rainfall-induced slope failures using the material point method. Proc. 12th Int. Symp. Landslides, Naples, Italy; 2016b. p. 2037–42.
Wang B., Vardon P.J., Hicks M.A. Rainfall-induced slope collapse with coupled material point method. Eng. Geol. 2018;239:1–12.
Wang B., Vardon P.J., Hicks M.A., Chen Z. Development of an implicit material point method for geotechnical applications. Comput. Geotech. 2016c;71:159–67.
Wang D., Wang B., Jiang Q., Guo N., Zhang W., He K. Large deformation slope failure—a perspective from multiscale modelling. Comput. Geotech. 2022a;150: 104886.
Wang D., Wang B., Yuan W., Liu L. Investigation of rainfall intensity on the slope failure process using GPU-accelerated coupled MPM. Comput. Geotech. 2023a;163:105718.
Wang D., Zhu H., Zhou G., Yu W., Wang B., Zhou W. Monitoring shear deformation of sliding zone via fiber Bragg grating and particle image velocimetry. J. Rock Mech. Geotech. Eng. 2024a;16(1):231–41.
Wang D.Y., Zhu H.H., Wang B.J., Shi B. Performance evaluation of buried pipe under loading using fiber Bragg grating and particle image velocimetry techniques. Measurement 2021a;186:110086.
Wang G., You G., Zhu J., Yu J., Gong X., Wu J. Investigations of changjing earth fissures, jiangyin, Jiangsu, China. Environ. Earth Sci. 2016d;75(6):502.
Wang J., Lin S.Q., Tan D.Y., Yin J.H., Zhu H.H., Kuok S.C. A novel method for integrity assessment of soil-nailing works with actively heated fiber-optic sensors. J. Geotech. Geoenviron. Eng. 2024b;150(8):04024063.
Wang L., Coombs W.M., Augarde C.E., Brown M., Knappett J., Brennan A., Richards D., Blake A. Modelling screwpile installation using the MPM. Procedia Eng. 2017; 175:124–32.
Wang L., Coombs W.M., Augarde C.E., Cortis M., Brown M.J., Brennan A.J., Knappett J.A., Davidson C., Richards D., White D.J., Blake A.P. An efficient and locking-free material point method for three-dimensional analysis with simplex elements. Int. J. Numer. Methods Eng. 2021b;122(15):3876–99.
Wang S., Zhao L., Liu Y. A concurrent multiscale method based on smoothed molecular dynamics for large-scale parallel computation at finite temperature. Comput. Methods Appl. Mech. Eng. 2023b;406:115898.
Wang Y., Gao D., Fang J. Finite element analysis of deepwater conductor bearing capacity to analyze the subsea wellhead stability with consideration of contact interface models between pile and soil. J. Pet. Sci. Eng. 2015;126:48–54.
Wang Y., Gao D., Meng C. Numerical simulation analysis on the lateral dynamic characteristics of deepwater conductor considering the pile-soil contact models. J. Mar. Sci. Eng. 2022b;10(10):1540.
Wang Y., Shi J., Ng C.W.W. Numerical modeling of tunneling effect on buried pipelines. Can. Geotech. J. 2011;48(7):1125–37.
Więckowski Z. The material point method in large strain engineering problems. Comput. Methods Appl. Mech. Eng. 2004;193(39–41):4417–38.
Wieckowski Z. Enhancement of the Material Point Method for Fluid-Structure Interaction and Erosion. Netherlands, Deltares: Delft; 2013.
Wols B.A., van Thienen P. Modelling the effect of climate change induced soil settling on drinking water distribution pipes. Comput. Geotech. 2014;55:240–7.
Wu B., Zhu H.H., Cao D.F., Liu X.F., Liu T.X. Fiber optic sensing-based field investigation of thermo-hydraulic behaviors of loess for characterizing land–atmosphere interactions. Eng. Geol. 2023;315:107019.
Xia G., Liu C., Xu C., Le T. Dynamic analysis of the high-speed and long-runout landslide

movement process based on the Discrete Element Method: a case study of the Shuicheng Landslide in Guizhou, China. Adv. Civ. Eng. 2021;1:8854194.
Xie T.C., Zhu H.H., Tan D.Y., Shukla S.K. Modeling pipe-soil interaction under surface loading using material point method. Tunn. Undergr. Space Technol. 2024a;147:105709.
Xie T.C., Zhu H.H., Zhang C.X., Liu W., Tan D.Y., Zhang W. Modeling pipe–soil interaction under lateral movement using material point method. J. Pipeline Syst. Eng. Pract. 2024b;15(1):04023058.
Xie T.C., Zhu H.H., Zhang C.X., Zhang W. Modeling strip footings on slopes using the material point method. Bull. Eng. Geol. Environ. 2023;82(4):99.
Xie X.C., Ceccato F., Zhou M.L., Zhang D.M. Hydro-mechanical behaviour of soils during water-soil gushing in shield tunnels using MPM. Comput. Geotech. 2022;145:104688.
Yang Y.S., Qiu L.C. MPM simulation of uplift resistance of enlarged base piles in sand. Soils Found. 2020;60(5):1322–30.
Ye X., Zhu H.H., Cheng G., Pei H.F., Shi B., Schenato L., Pasuto A. Thermo-hydro-poro-mechanical responses of a reservoir-induced landslide tracked by high-resolution fiber optic sensing nerves. J. Rock Mech. Geotech. Eng. 2024;16(3):1018–32.
Yerro A., Alonso E.E., Pinyol N.M. The material point method for unsaturated soils. Geotechnique 2015;65(3):201–17.
Yerro A., Alonso E.E., Pinyol N.M. Run-out of landslides in brittle soils. Comput. Geotech. 2016;80:427–39.
Yerro A., Girardi V., Martinelli M., Ceccato F. Modelling unsaturated soils with the Material Point Method. A discussion of the state-of-the-art. Geomech. Energy Environ. 2022;32:100343.
Yerro A., Soga K., Bray J. Runout evaluation of Oso landslide with the material point method. Can. Geotech. J. 2019;56(9):1304–17.
Yildizdag M.E. Numerical modeling and simulation of material extrusion-based 3-D printing processes with a material point method framework. Continuum Mech. Therm. 2023;1–18.
Yimsiri S., Soga K., Yoshizaki K., Dasari G.R., O'Rourke T.D. Lateral and upward soil-pipeline interactions in sand for deep embedment conditions. J. Geotech. Geoenviron. Eng. 2004;130(8):830–42.
Ying C., Zhang K., Wang Z.N., Siddiqua S., Makeen G.M.H., Wang L. Analysis of the run-out processes of the Xinlu Village landslide using the generalized interpolation material point method. Landslides 2021;18:1519–29.
York A.R., Sulsky D., Schreyer H.L. Fluid–membrane interaction based on the material point method. Int. J. Numer. Methods Eng. 2000;48(6):901–24.
Yost K., Martinelli M., Yerro A., Green A., de Lange W. Addressing complexities in MPM modeling of calibration chamber cone penetrometer tests in homogenous and highly interlayered soils. Comput. Geotech. 2023;158:105378.
Yost K.M., Yerro A., Green R.A., Martin E., Cooper J. MPM modeling of cone penetrometer testing for multiple thin-layer effects in complex soil stratigraphy. J. Geotech. Geoenviron. Eng. 2022;148(2):04021189.
Yu J., Zhao J., Liang W., Zhao S. Multiscale modeling of coupled thermo-hydro-mechanical behavior in ice-bonded granular media subject to freeze-thaw cycles. Comput. Geotech. 2024;171:106349.
Yuan W.H., Wang B., Zhang W., Jiang Q., Feng X.T. Development of an explicit smoothed particle hydrodynamics method for geotechnical applications. Comput. Geotech. 2019a;106:42–51.
Yuan W.H., Wang H.C., Zhang W., Dai B.B., Liu K., Wang Y. Particle finite element method implementation for large deformation analysis using Abaqus. Acta Geotech 2021;16:2449–62.
Yuan W.H., Zhang W., Bai B., Wang Y. Application of the particle finite element method for large deformation consolidation analysis. Eng. Comput. 2019b;36:3138–63.
Yuan W.H., Zheng H., Zheng X., Wang B., Zhang W. An improved semi-implicit material point method for simulating large deformation problems in saturated geomaterials. Comput. Geotech. 2023;161:105614.
Zabala F., Alonso E.E. Progressive failure of Aznalcóllar dam using the material point method. Geotechnique 2011;61(9):795–808.
Zdravković L. Finite Element Analysis in Geotechnical Engineering: Theory. Thomas Telford; 1999.
Zeng Z., Zhang H., Zhang X., Liu Y., Chen Z. An adaptive peridynamics material point method for dynamic fracture problem. Comput. Methods Appl. Mech. Eng. 2022;393:114786.
Zhan Z.Q., Zhou C., Liu C.Q., Ng C.W.W. Modelling hydro-mechanical coupled behaviour of unsaturated soil with two-phase two-point material point method. Comput. Geotech. 2023;155:105224.
Zhang C., Zhu H., Li H. Modeling pipe-soil interaction under vertical downward relative offset using B-spline material point method. J. Rock Mech. Geotech. Eng. 2023a;15(6):1520–34.
Zhang C.X., Zhu H.H., Zhang W., Li H.J., Liu W. Modeling uplift failure of pipes buried in sand using material point method. Tunn. Undergr. Space Technol. 2022a;119:104203.
Zhang D.M., Xie X.C., Zhou M.L., Huang Z.K., Zhang D.M. An incident of water and soil gushing in a metro tunnel due to high water pressure in sandy silt. Eng. Fail. Anal. 2021;121:105196.
Zhang D.Z., Ma X., Giguere P.T. Material point method enhanced by modified gradient of shape function. J. Comput. Phys. 2011;230(16):6379–98.
Zhang G., Zhang J. State of the art: mechanical behavior of soil–structure interface. Prog. Nat. Sci. 2009;19(10):1187–96.
Zhang H., Yang J., Wang L., Xu Y., Lan S., Luo J., Chang Z. Experimental and numerical investigation on failure mechanism of expansive soil subgrade slope. Sci. Rep. 2023b;13:19795.
Zhang H.W., Wang K.P., Chen Z. Material point method for dynamic analysis of saturated porous media under external contact/impact of solid bodies. Comput. Methods Appl. Mech. Eng. 2009;198(17–20):1456–72.
Zhang P., Liu L.L., Zhang S.H., Cheng Y.M., Wang B. Material point method-based two-dimensional cohesive-frictional slope stability analysis charts considering depth coefficient effect. Bull. Eng. Geol. Environ. 2022b;81(5):206.
Zhang R., Gomaa S.M., Hussein M., Zayed T., Meguid M. Review of numerical approaches used in soil-pipe interaction analysis of water mains. Transp. Geotech. 2023c;42:101008.
Zhang W., Maeda K., Saito H., Li Z., Huang Y. Numerical analysis on seepage failures of dike due to water level-up and rainfall using a water–soil-coupled smoothed particle hydrodynamics model. Acta Geotech 2016a;11:1401–18.
Zhang X., Chen Z., Liu Y. The Material Point Method: A Continuum-Based Particle Method for Extreme Loading Cases. Academic Press; 2016b.
Zhao L., Qiao N., Huang D., Zuo S., Zhang Z. Numerical investigation of the failure mechanisms of soil–rock mixture slopes by material point method. Comput. Geotech. 2022a;150:104898.
Zhao S., Chen H., Zhao J. Multiscale modeling of freeze-thaw behavior in granular media. Acta Mech. Sin. 2023a;39(1):722195.
Zhao S., He S., Li X., Deng Y., Liu Y., Yan S., Bai X., Xie Y. The Xinmo rockslide-debris avalanche: an analysis based on the three-dimensional material point method. Eng. Geol. 2021;287:106109.
Zhao S., Zhao J., Liang W., Niu F. Multiscale modeling of coupled thermo-mechanical behavior of granular media in large deformation and flow. Comput. Geotech. 2022b;149:104855.
Zhao S., Zhu L., Liu W., Li X., He S., Scaringi G., Tang X., Liu Y. Substratum virtualization in three-dimensional landslide modeling with the material point method. Eng. Geol. 2023b;315:107026.
Zhao Y., Choo J., Jiang Y., Li L. Coupled material point and level set methods for simulating soils interacting with rigid objects with complex geometry. Comput. Geotech. 2023c;163:105708.
Zhao Y., Choo J., Jiang Y., Li M., Jiang C., Soga K. A barrier method for frictional contact on embedded interfaces. Comput. Methods Appl. Mech. Eng. 2022c;393:114820.
Zheng X., Wang S., Yang F., Yang J. Material point method simulation of hydro-mechanical behaviour in two-phase porous geomaterials: a state-of-the-art review. J. Rock Mech. Geotech. Eng. 2024;16(6):2341–50.
Zhou Z., Yin Z.Y., He G.F., Zhang P., Jiang M. The potential of a multi-fidelity residual neural network based optimizer to calibrate DEM parameters of rock-like bonded granular materials. Comput. Geotech. 2024;168:106137.
Zhu H.H. Engineering geological interfaces: from multivariate characterization to evolution mechanism. Bull. Geol. Sci. Technol. 2023;42(1):1–20. (in Chinese).
Zhu H.H., Xie T.C., Zhang W., Shukla S.K. Numerical simulations of a strip footing on the soil slope with a buried pipe using the material point method. Int. J. GeoMech. 2023;23(11):04023190.
Zhu H.H., Yin J.H., Yeung A.T., Jin W. Field pullout testing and performance evaluation of GFRP soil nails. J. Geotech. Geoenviron. Eng. 2011;137(7):633–42.
Zhu Y., Ishikawa T., Zhang Y., Nguyen B.T., Subramanian S.S. A FEM-MPM hybrid coupled framework based on local shear strength method for simulating rainfall/runoff-induced landslide runout. Landslides 2022;19(8):2021–32.
Zwanenburg W., Wittekoek R., Martinelli M., Alderlieste E. The effect of finite layer thickness; a validation of MPM analysis by centrifuge testing. Proc. 10th European Conf. On Numerical Methods in Geotechnical Engineering; 2023. p. 1–6.

Dr. Honghu Zhu is currently Professor at the School of Earth Sciences and Engineering and Dean of the Institute of Earth Exploration and Sensing, Nanjing University, China. He holds a PhD in Geotechnical Engineering from the Hong Kong Polytechnic University. His research interests primarily lie in fiber optic monitoring and stability analysis of geoengineering issues, with a particular emphasis on geo-interface behaviors. His research outputs have been transformed into practical applications across multiple research projects, such as landslide monitoring in the Three Gorges Reservoir Area, debris flow prevention in the Wenchuan Earthquake Zone, and structural health monitoring of the Pearl River Delta water conveyance tunnel. Over the past decade, he has co-authored 2 books, 12 patents, and over 100 journal and conference papers. In recognition of his contributions to engineering geology and geotechnics, he was awarded the 1st-class Prize of National Scientific & Technological Progress Award of China in 2018 and was granted funding from the National Science Fund for Distinguished Young Scholars in 2022. He serves as an editorial board member of the *Journal of Rock Mechanics and Geotechnical Engineering* (*JRMGE*) and five other international journals.